
The Oasis Effect

Evaluating intrinsic biophysical
mechanism theory and its implications
for sustainable water management in
Zhangye, Gansu, China

Sophie A. Ruehr

A Senior Thesis presented to the faculty of the Department of Geology and
Geophysics, Yale University, in partial fulfillment of the Bachelor's Degree.

Professor Xuhui Lee, advisor
Professor Ronald Smith, second reader

In presenting this thesis in partial fulfillment of the Bachelor's Degree from the Department of Geology and Geophysics, Yale University, I agree that the department may make copies or post it on the departmental website so that others may better understand the undergraduate research of the department. I further agree that extensive copying of this thesis is allowable only for scholarly purposes. It is understood, however, that any copying or publication of this thesis for commercial purposes or financial gain is not allowed without my written consent.

Sophie Ruehr, May 2, 2018

Abstract: Oases support life in harsh desert environments where water is scarce. Climate change, population growth and economic development threaten the health of these ecosystems, which are important centers of economic and agricultural activity in arid regions around the world. This study employs remote sensing analysis and intrinsic biophysical mechanism (IBPM) theory to provide insight on oasis-desert energy and hydrology dynamics, as well as recent trends in land use change in Zhangye, Gansu, China. Remote sensing analysis provides an estimate of increased water demand due to expansion of agricultural areas surrounding the city. Ground, latent, and sensible heat flux, as well as radiation data from paired desert and oasis meteorological monitoring sites from the HiWATER project are analyzed. Correlation analyses are performed to assess the effects of wind speed, wind direction and insolation on the oasis effect. IBPM theory is shown to successfully model the observed oasis effect at noon and midnight in summer 2013. Insolation and wind speed are shown to have significant impacts on the surface temperature oasis effect. The implications of this study are useful for sustainable water management in arid agricultural regions throughout the world.

Keywords: Oasis effect; energy partitioning; semi-arid region; IBPM theory.

1 INTRODUCTION	2
1.1 OASES & DESERTS	2
1.2 LITERATURE REVIEW	4
2 DATA & STUDY AREA	6
2.1 ZHANGYE, GANSU, CHINA	6
2.2 CURRENT WATER MANAGEMENT PRACTICES IN ZHANGYE	9
2.3 HiWATER DATA PROJECT	11
3. METHODS	11
3.1 LAND USE CHANGE ANALYSIS & REMOTE SENSING	11
3.2 FIELD SITE, DATA AND STATISTICAL ANALYSIS OF THE OASIS EFFECT	13
3.3 IBPM THEORY: A MECHANISTIC APPROACH	15
3.4 CORRELATION ANALYSES	17
3.4.1 Wind analysis	18
3.4.2 Cloudy-day analysis	18
4. RESULTS & DISCUSSION	19
4.1 LAND USE CHANGE ANALYSIS & REMOTE SENSING	19
4.2 A STATISTICAL DEPICTION OF THE OASIS EFFECT	22
4.3 IBPM THEORY RESULTS	24
4.4 CORRELATION ANALYSES RESULTS	28
4.4.1 Wind speed and direction	29
4.4.2 Cloudy-day analysis results	32
5. CONCLUSION	32
ACKNOWLEDGEMENTS	34
BIBLIOGRAPHY	34

1 Introduction

1.1 Oases & deserts

Increasing demand for fresh water in semi-arid and arid regions around the world has resulted in extreme ecological degradation, lack of access to fresh water and desertification. Semi-arid and arid regions represent 30% of the global terrestrial surface area and are expanding (Scanlon et al., 2006). Oases are important sources of fresh water in arid and semi-arid regions despite their small size. For example, oases support more than 95% of people living in China's arid regions even though oases make up less than 5% of the total area of arid regions in China (Li et al., 2016). Furthermore, oases are "hot spots of climate change" as they are threatened by desertification. Desert regions are expected to expand to up to 50% of the global land area by the end of this century (Li et al., 2016). With population growth, climate change and economic development, sustainable water management and agriculture in arid and semi-arid regions is more important now than ever, as Li et al. (2016), Hao et al. (2016) and Micklin (1988) have shown.

Detailed models of watershed dynamics and rigorous methodology for monitoring oasis hydrology are crucial components in sustainable agriculture and water management in arid and semi-arid regions (Li et al., 2016). However, many aspects of these systems are unresolved. As an IPCC report suggests, "Regional detection and attribution of land degradation and desertification to climate influences is challenging due to the occurrences of multiple other influences. These influences include increased extensive and intensive agriculture, deforestation, overgrazing, inappropriate land use change and population pressures especially on environmentally fragile lands subject to overuse" (Working Group III, 2017). Atmospheric boundary-layer meteorology and land use change analysis are increasingly relevant in providing mechanistic explanations for observed phenomena. This study investigates one such phenomenon, the oasis effect, and attempts to model the effect using data from Zhangye, Gansu, China.

The oasis effect is defined by the difference in air temperature between the oasis and desert. The oasis typically has a lower surface temperature than the surrounding desert, resulting in a negative oasis effect. Along with the oasis effect, several other atmospheric boundary layer effects are observed in desert-oasis systems. A temperature inversion is observed over the oasis, as air temperature over the two sites equilibrate with height. As rapid advection occurs over the desert, wet and cooler air from the oasis moves outwards into the desert, distributing water vapor that maintains desert vegetation (Kai et al., 1997). The warm, dry air rising from the desert area moves

above the oasis, creating a stable mesoclimate and a net flux of water vapor from the oasis into the desert (Li et al., 2016). Previous literature has established that the oasis effect occurs due to a large latent heat flux over the oasis, where water evaporates and takes up heat in its phase change, cooling the oasis. Figure 1, adapted from Kai et al. (1997), shows the varying magnitudes of latent and sensible heat flux over the desert, as well as the inversion over the oasis, for summer 2013. It

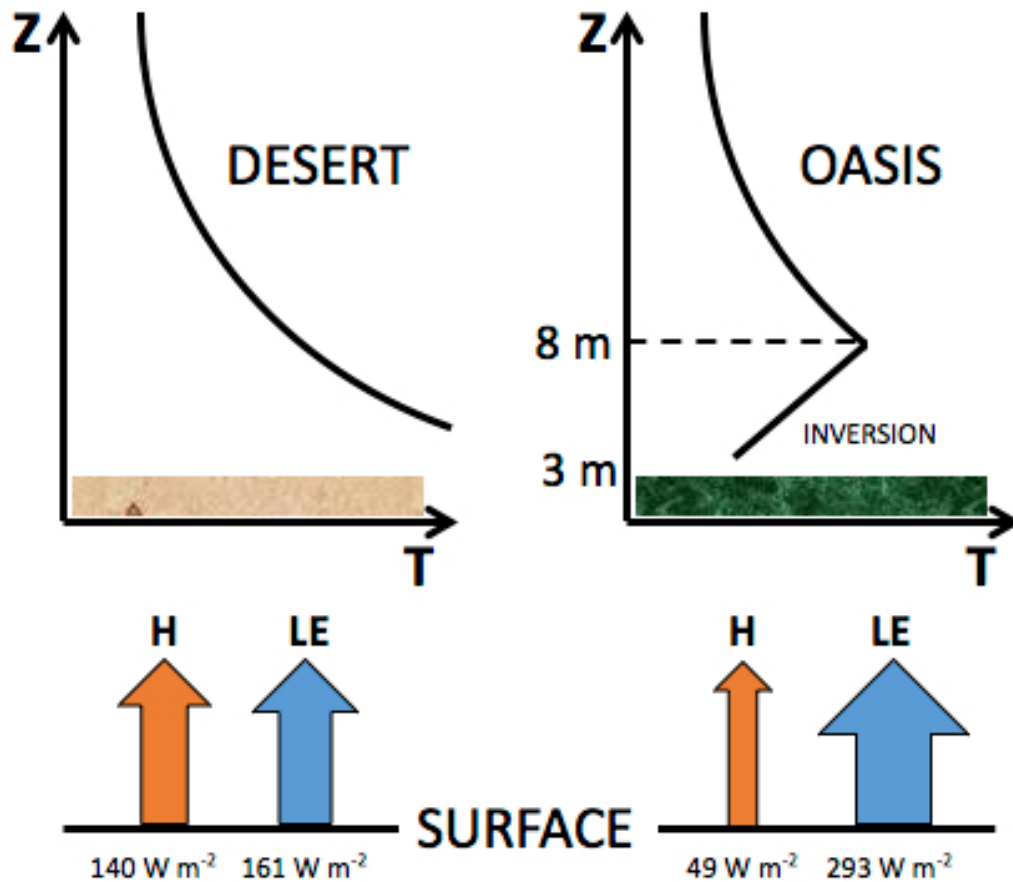


Figure 1: Diagram of the oasis effect. Over the desert, sensible and latent heat fluxes are positive and upwards. A large upwards latent heat flux cools the oasis. Over the oasis, an inversion occurs until 8m, producing a cooler surface temperature than in the desert. Values are summer 2013 noontime averages from data in this study. Modified from Kai et al. (1997).

also shows the temperature inversion observed over the oasis. In summary, the oasis can be described as a ‘cool-wet island’ and the desert as a ‘warm-dry sea.’

This study is divided into four sections. First, remote sensing analysis is applied to contextualize recent land use change in Zhangye. Secondly, a statistical description of seasonal and hourly oasis effects is developed from data collected in 2013. Third, intrinsic biophysical

mechanism theory developed by Lee et al. (2011) and Wang et al. (2018) is employed to mechanistically model the sign and magnitude of the observed oasis effect. Finally, correlation analysis is performed to determine the impact of wind speed, wind direction and atmospheric clarity on the oasis effect. All analyses were completed with data from the HiWATER metrological monitoring project based in the Heihe River Basin in 2013. The goal of this study is to gain insight on processes that affect the long-term stability of desert-oasis ecosystems and provide meaningful context for watershed development and management strategies in China's arid regions and beyond.

With generous support from the Karen L. Von Damm '77 Undergraduate Research Fellowship in Geology & Geophysics, I was able to visit my field site. While in Zhangye, I learned about the methodology used in collecting meteorological data, met with scientists who work on the HiWATER watershed monitoring project, and collected ground truth measurements to verify my remote sensing analysis. The visit also provided me with an opportunity to better understand the context of my senior thesis in terms of local economic and political concerns and appreciate how my project continues ongoing research on water management in arid regions.

1.2 Literature review

The following literature review presents a brief description of recent research regarding the oasis effect, IBPM theory, and hydrology in semi-arid and arid regions.

The oasis effect was first observed in the Heihe River Basin by Kai et al. (1997). Using data collected during the Heihe River Basin Field Experiment in June 1991, the authors model the oasis effect using ground, latent and sensible heat fluxes balanced by net radiation. Data from 5 clear-weather days were selected for the analysis. A 7°C horizontal temperature gradient between the desert and oasis was observed during the afternoon. The authors found that an inversion occurs around 8 m over the oasis station during afternoon hours, implying a downward sensible heat flux. Over the desert, there was no observed inversion and the sensible heat flux was positive. Kai et al. observed that wind speed affected sensible heat fluxes. Larger wind speed was correlated to a decrease in sensible heat flux over the oasis and an increase in sensible heat flux over the desert, implying that the oasis effect is more intense with increased wind speed. The authors concluded that the oasis effect arises primarily from a large latent heat flux over the oasis.

As Hao et al. (2016) show, the oasis effect is greatest in the summer months. During the growing season, irrigation is most intensive, resulting in a larger latent heat flux over the oasis due

to the increased availability of water. Over the 50-year period of the study, temperatures in the Tarim Basin in North China have been consistently rising at a quicker rate compared to other areas of China. Hao et al. show that this trend is due to a combination of two factors. The temperatures across the basin are in fact rising; however, the oasis effect is also diminishing over time, resulting in a larger rate of temperature rise within the oasis. The authors conclude that the diminishing oasis effect is due to decreasing wind speed over Northwest China, expansion of arid land and new water-saving agricultural techniques that limit the amount of water used in irrigation, and therefore evapotranspiration in the oasis.

Monthly evapotranspiration by land cover

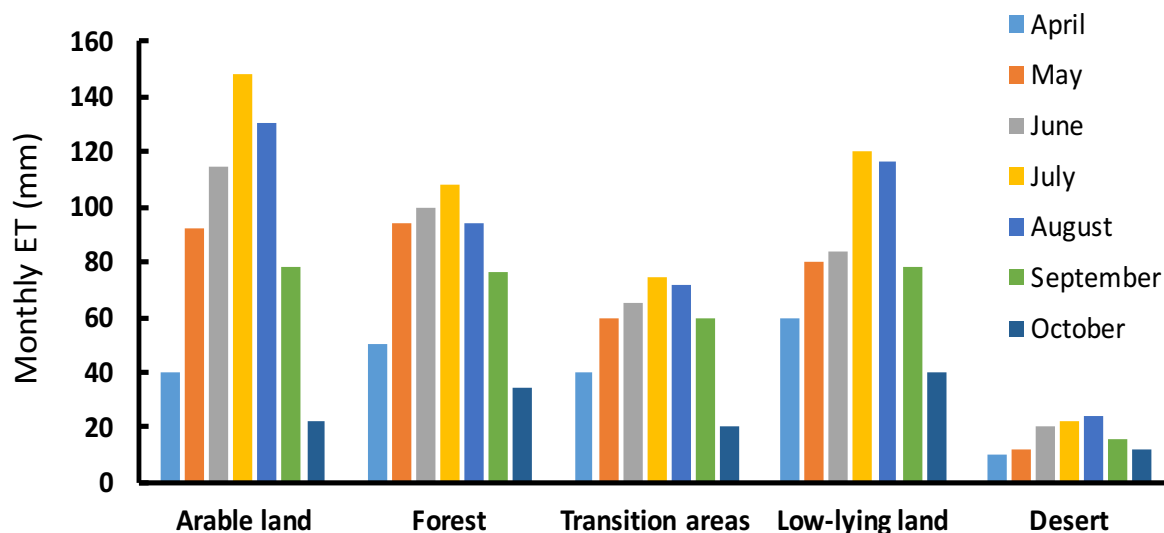


Figure 2: Monthly evapotranspiration rates (ET) for five land cover classes in spring, summer and fall. Largest rates of ET occur over arable land during July and August. Smallest rates of ET occur over the desert throughout the year. The desert is also least variable in its ET rates. Figure adapted from Liang & Huang (2015).

Taha et al. (1991) used data collected from a meteorological monitoring network on a transect through an orchard in California. They analyzed the impact of the canopy on wind speed and temperature both up- and downwind of the orchard. The authors observed a nighttime heat island and daytime oasis effect in the canopy, resulting from spatially-differentiated atmospheric heating and cooling rates. Regression analysis was applied to find an empirical relationship between wind speed and oasis effects. The authors showed that wind speed increased temperature depression in the canopy during the day.

Potchter et al. (2008) studied the diurnal dynamics of an artificial oasis and its impacts on the oasis effect in Israel. Using data from 4 consecutive days of summer over 3 years, the authors observed that the magnitude of the oasis effect was dependent on vegetation type. Surface temperature was shown to have the highest range in the desert and the smallest range in the irrigated forest. The authors found that higher wind speed decreased the oasis effect (in contrast to Kai et al. (1997)) and a larger relative humidity decreased the oasis effect.

Lian & Huang (2015) used LANDSAT 8 satellite images and the METRIC model to quantify evapotranspiration over a heterogeneous landscape in an arid region of Northwest China. As the oasis landscape is patchy (there are many land uses in a small area), the authors focused on extreme pixels that were significantly impacted by sensible heat flux estimation. Their analysis showed that evapotranspiration values peak in the summer due to a large amount of water supply and increase evaporation, with the greatest seasonal variation in evapotranspiration observed in arable land and the smallest amount of evapotranspiration in the desert (Figure 2). Their estimations of evapotranspiration rates over desert and oasis patches is used to approximate increased water consumption due to agricultural expansion in this study.

Finally, Lee et al. (2011) and Wang et al. (2018) applied IBPM theory to analyze temperature differences between two land cover types. Lee et al. (2011) showed that IBPM theory successfully models the impact of deforestation on surface air temperature in mid- to high latitudes. Wang et al. (2018) showed that IBPM theory correctly predicts the observed temporal variations of surface temperature in a case of afforestation in the Kubuqi Desert, Inner Mongolia, China. The current study relies on the methodologies developed by Lee et al. (2011) and Wang et al. (2018) to evaluate the ability of IBPM theory to successfully model the oasis effect, with implications for IBPM theory's ability to apply to a variety of ecosystems and heterogeneous landscapes.

2 Data & Study area

2.1 Zhangye, Gansu, China

The Heihe River, or the Black River, is the second longest inland river in China. The current population of Zhangye city is over 1.2 million, with an additional 770,000 residents in the river basin. During the era of the Silk Road, Zhangye was a major trading post and rest stop for travelers and merchants (Meng, 2009). The area has also long been an agricultural center. In recent years, the majority of agricultural production has consisted of corn for seed. Zhangye lies in the transition

zone between the westerlies and summer monsoon (Wen et al., 2016), and the Heihe River is fed by snowmelt from the Qilian Mountains that surround the basin.

Precipitation and relative humidity remain low throughout the year. As shown by Figure 3, the majority of precipitation falls in the summer months (June, July and August), reaching a maximum of approximately 30 mm in August. The fall, spring and winter months are extremely dry, with precipitation values ranging from 1 to 3 mm (Kai et al., 1997). Relative humidity varies from 40% to 60%, with drier conditions in March, April and May. Temperatures reach their peak in July (with daily highs of 30°C) and minimum in December and January (with daily highs of 0°C).

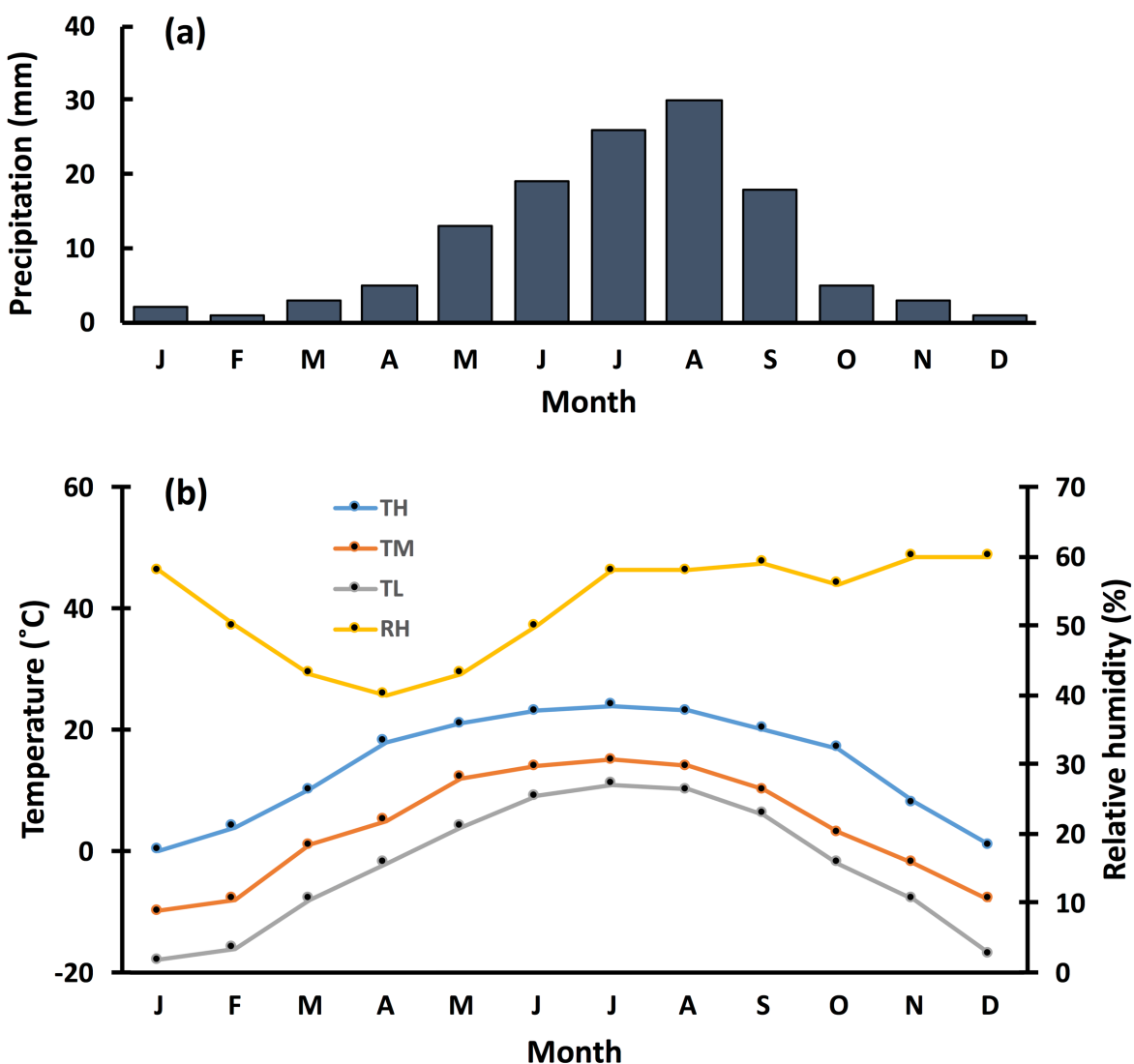


Figure 3: (a) Mean precipitation, (b) mean relative humidity (RH), mean air temperature (TM), mean daily temperature maximum (TH) and minimum (TL) temperatures in Zhangye, Gansu, China. Values from meteorological data collected from 1951 to 1980. Figure adapted from Kai et al. (1997)

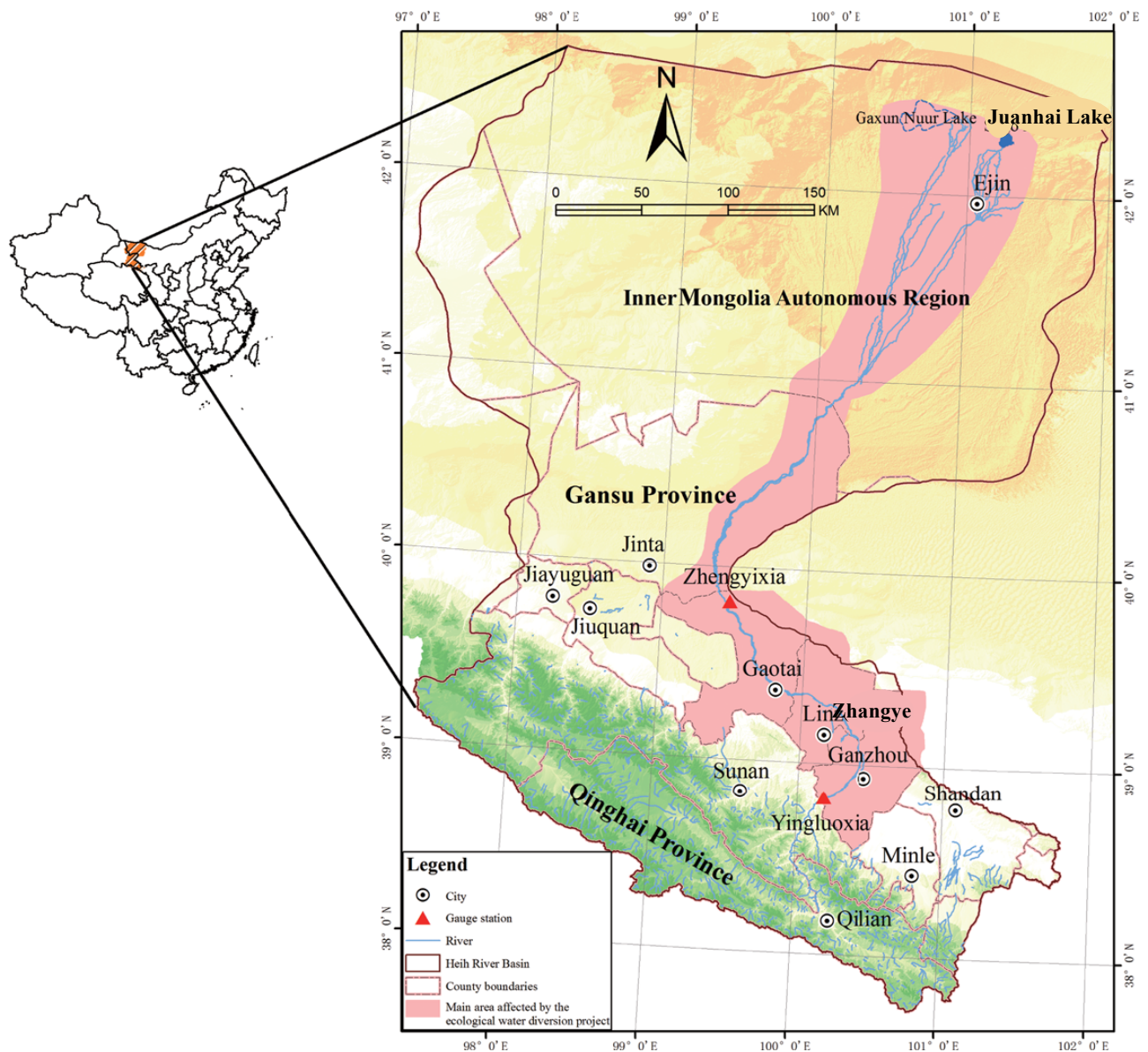


Figure 4: The Hexi Corridor and the Heihe River watershed monitored by HiWATER meteorological stations network (shaded in pink). The Heihe River (blue) runs from the Qilian Mountains (green) northward, through Zhangye and terminating in two terminal lakes. Figure from Li et al. (2014).

Water is a vital yet scarce resource in Zhangye. 81% of the water in the Heihe River is used by agriculturalists in the area surrounding Zhangye, and recent population growth has put more strain on water resources (Wang et al., 2015). 50% of farmland in Zhangye is fed by irrigation and more than 90% of water goes to agriculture in the region (Xu et al., 2014). Recently, industry has entered the region, which has led to dramatic economic development and a 13% increase in gross domestic product for the area in 2000 alone (Peng et al., 2007). The river, before the 1990s when water usage increased dramatically, fed several wetlands and discharged into the Juanhai Lake to the

north of Zhangye, as shown in Figure 4. With increasing demand on water resources, the volume of water in the Heihe River downstream from Zhangye decreased dramatically by 1995, resulting in significant impacts downstream. The Juanhai Lake dried up and the *Populus euphratica* near the lake largely died. In 1995, the Lanzhou Institute of Desert Research at the Chinese Academy of Sciences assessed the Heihe River watershed and suggested an intensive reallocation of water resources to ensure an increase of flow in the downstream reaches of the river. Their suggestions were implemented, and steady recovery of *P. euphratica* forests and the rehabilitation of the Juanhai Lake are testaments to the success of this project (Cheng et al., 2007). However, with the rapid increase in population and economic development in the past 20 years, sustainable water management is still a major concern for the city (Cheng et al., 2007; Li et al., 2011).

Recent studies have shown that global warming may affect the climate in Gansu province by shifting summer weather from a warm-dry to a warm-wet climate. This transition may result in increased precipitation in Gansu Province (Cheng et al., 2014). However, the glaciers in the Quilian mountain range, whose melt water feeds the Heihe River and irrigation projects (Cheng et al., 2007), have been steadily decreasing in mass since the 1970s (Xiao et al., 2007). Agricultural areas have migrated upstream, where water resources are more available, and farmland has expanded considerably in the past 20 years alone (this study). With a growing population, climate change and expanding agriculture, the future of water availability in the region is uncertain. This uncertainty limits the effectiveness of water management and may lead to harmful impacts on human activities and the ecosystems supported by the Heihe River.

2.2 Current water management practices in Zhangye

Water in Zhangye and its outlying agricultural areas is currently divided by district according to the number of farmers living there. Water infrastructure, including irrigation canals, is maintained and controlled by Water User Associations (WUAs), composed of elected representatives. Water user associations (WUAs) are user-based and participatory approaches to improving water delivery, crop production and involving farmers in irrigation management. In order to improve management, these groups pool financial, technical and human resources to maintain and operate irrigation systems (Xu et al., 2014). Changes in river flow, labor availability and the complexity of the irrigation has resulted in difficulties in operating WUAs. The amount of water is allocated per household, based on family size and size of arable land (Xu et al., 2014).

While visiting Zhangye, I was able to observe the flood irrigation around poplar trees and an activated irrigation canal (Figure 5).

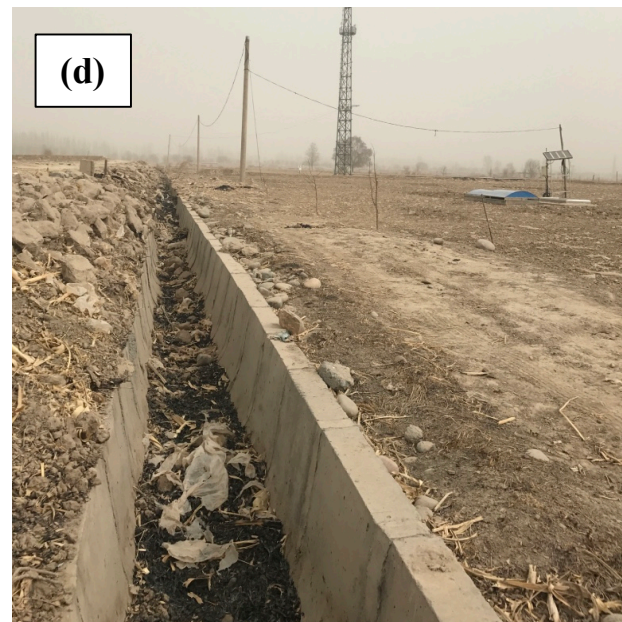
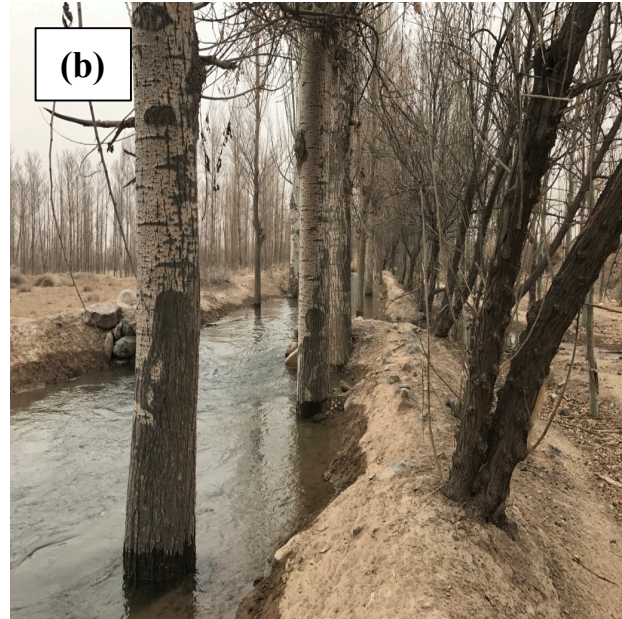
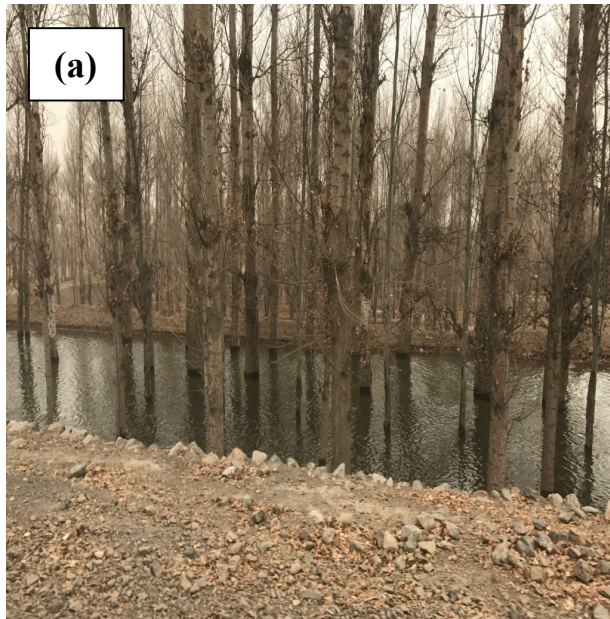


Figure 5: Images from the author's trip to Zhangye in winter 2018. (a) and (b) Poplar flood irrigation. This method of irrigation is also used for the corn crop at the Daman oasis station. (c) An active irrigation canal near the desert steppe station. (d) An inactive irrigation canal near the Daman oasis station.

2.3 HiWATER data project

The Heihe Watershed Allied Telemetry Experimental Research (HiWATER) project was launched in May 2012 in the Heihe River Basin to study the hydrology of arid ecosystems. HiWATER aims to “provide fundamental theory and technical support for water security, ecological security and sustainable development in inland river basins,” which make up 11.4% of the world’s land area (Li et. al, 2013). The stations monitored glacial flow in the mountains, water usage in an artificial agricultural oasis in Zhangye, and river flow volume downstream from the city. The stations are equipped with eddy covariance systems, large aperture scintillometers, cosmic-ray neutron probes and wireless sensor networks. There have also been aerial surveys of the area conducted by drones and more intensive, short-term analyses performed in various ecosystems along the Heihe River (including alpine zones, wetland areas, arid regions, and natural and artificial oases). The HiWATER project has resulted in dozens of publications on arid-region hydrology and meteorology due to the fact that the data is freely accessible online. A main goal of the project (and data engineering accomplishment) has been to provide accurate, accessible data for collaborative analysis and research.

3. Methods

To gain greater insight on the oasis effect and its agricultural context in Zhangye, four analyses are performed. First, remote sensing analysis is applied to contextualize recent land use change in Zhangye. Secondly, a statistical description of seasonal and hourly oasis effects is developed. Third, data from paired desert and oasis stations from the HiWATER project are used to analyze IPBM theory and produce a mechanistic model of the oasis effect. Finally, a correlation analysis of the impacts of wind speed, wind direction and insolation on oasis effects is conducted.

3.1 Land use change analysis & remote sensing

Remote sensing can provide helpful spatial and temporal understandings of land uses. This analysis of recent land use change in Zhangye can be used to approximate water consumption increase in the past 20 years, as well as quantify urban and agricultural expansion. This analysis is performed using Environment for Visualizing Images (ENVI) software and 3 satellite images from LANDSAT satellites. The three images were captured on July 9, 1991, July 23, 2002 and July 21, 2013. The standardization of acquisition date accounts for seasonal variation. The images were

taken at 3:57 GMT, or 10:57 a.m. local time in Zhangye. Table 1 shows details about the three images, which are largely cloud-free.

Table 1.

Date	Satellite
July 9, 1991	LANDSAT 4-5
July 23, 2002	LANDSAT 4-5
July 21, 2013	LANDSAT 8

The three images were subset to a region that captured Zhangye and its surrounding agricultural areas, measuring 70x62 km² and centered on 38°47'36.56"N, 100°20'43.41"E. Top-of-atmosphere correction and quick atmospheric correction algorithms were run on ENVI to remove distortion due to water vapor (clouds) in the stratosphere. The normalized difference vegetation index (NDVI) was taken according to the following equation:

$$NDVI = \frac{NIR - VIS}{NIR + VIS}$$

where *NIR* is the near-infrared radiation band (0.85-0.87 μm) and *VIS* is the red radiation band (0.6-0.7 μm). An older image (e.g. 1991) was then subtracted from a newer image (e.g. 2013), resulting in an image of the difference in NDVI between the two years.

NDVI is a helpful indicator of vegetation, as vegetation strongly absorbs red light and strongly reflects NIR radiation. Therefore, vegetated areas have high NDVI values whereas barren or urban areas have low NDVI values. A raster slice was applied to the image of the difference of NDVI values, with bright red representing a large decrease in NDVI values between the two years (values from -0.22 to -1.58) and bright green representing a large increase in NDVI values (from +0.45 to +1.8). Figure 8 shows the results of this process and Table 2 contains the quantification of these results, which are discussed in more detail below.

As Liang & Huang (2015) showed, oasis areas have a seasonal evapotranspiration rate (ET) of 800 to 1,200 mm. Desert areas have ET values of >200 mm. As a conservative estimate, the evapotranspiration beyond baseline required in an irrigated area is approximated to be 600 mm. This value is multiplied by the total new agricultural area between 1991 and 2013 to approximate the increased demand for water in the study area.

3.2 Field site, data and statistical analysis of the oasis effect

The data used in this study were taken primarily from the Daman Oasis Super Station (located at 100.372° E, 38.856° N, with an elevation of 1556 m) and Huazhaizi Desert Steppe Station (located at 100.319° E, 38.765° N, with an elevation 1731m). Both stations were designed and constructed for the HiWATER project in 2013. See Figure 6 for a photo of the field sites (and me visiting them). The stations were 11 km apart, with the Daman station located in the middle of a corn field approximately 10 km southwest of the center of Zhangye city and the desert station located 11 km to the southwest of the Daman oasis station and approximately 21 km southwest of the center of Zhangye.

The oasis station is located in a corn field. The vegetation reaches approximately 3 m during the summer, and flood irrigation, with water from the Heihe River directed to the field via irrigation canals, waters the crops. For images of the desert and oasis stations, see Figure 6. Recently,

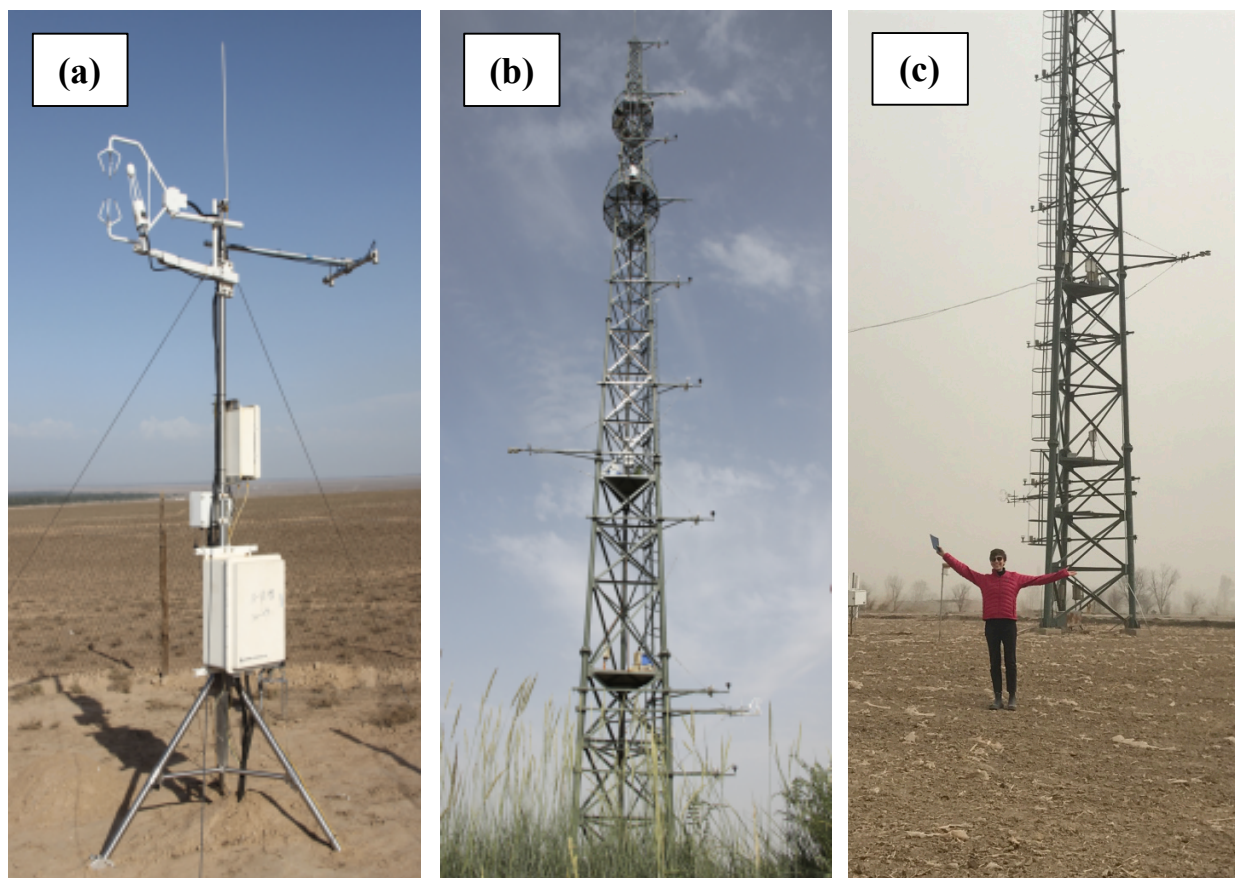


Figure 6: (a) Huazhaizi Desert Steppe and (b) Daman Oasis Superstation site images from the HiWATER meteorological monitoring project's website. Note the sparse vegetation at the desert site and tall corn crop at the oasis site. (c) Oasis station in March 2018 during dust storm (author included solely for purposes of scale).

greenhouses have become popular near the oasis station for growing vegetables and flowers (Figure 7). The desert station is located in a desert steppe area with sparse vegetation (Figure 7).

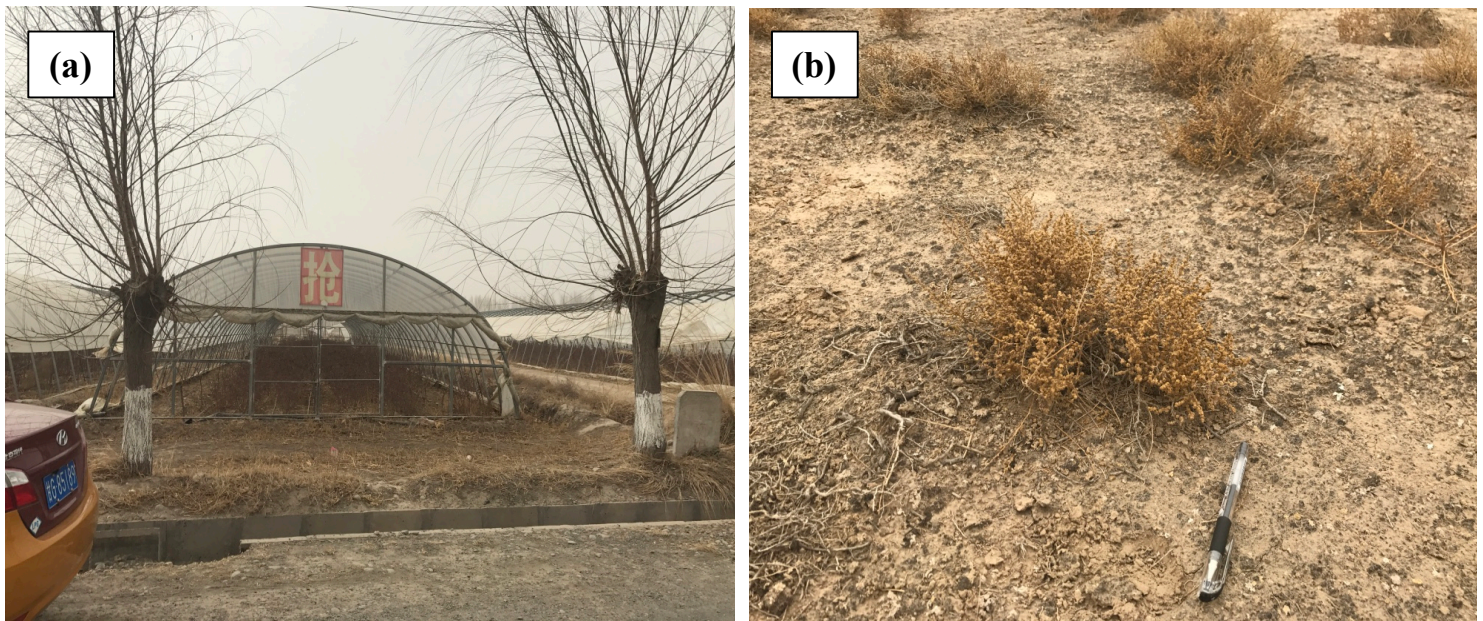


Figure 7: (a) Green houses are increasingly common in the fields surrounding Zhangye. Green houses are used to grow fruits, vegetables and flowers, which are more valuable than corn for seed. These greenhouses may complicate remote sensing analysis. (b) Sparse vegetation at the desert station with pen for scale. Images from the author's trip to Zhangye in March 2018.

The datasets from the oasis and desert stations included the following variables at half-hourly measurements for the calendar year 2013: heat flux (ground, latent and sensible), relative humidity, wind speed at several heights (up to 8 m at the desert station and 40 m at the oasis station), temperature, precipitation, radiation (incoming and outgoing long-wave and short-wave), soil moisture, surface temperature and pressure (Li et al., 2013). The data files are publicly accessible on and can be downloaded freely from the HiWATER website. Unphysical values are marked by an algorithm developed by meteorologists at Beijing Normal University (Liu et al., 2011) and rejected.

The data were averaged over summer, fall, winter and spring to distinguish diurnal temperature, humidity and heat flux trends at the two sites. The oasis effect was calculated to one standard deviation (Figure 10). Seasonal albedo was derived from the ratio of incoming shortwave to outgoing shortwave incoming radiation (Figure 11).

3.3 IBPM theory: a mechanistic approach

Following Wang et al. (2018), Lee et al. (2011) and Professor Xuhui Lee's *Fundamentals of Boundary-Layer Meteorology* (2018), intrinsic biophysical mechanism (IBPM) theory was applied as a mechanistic model of the oasis effect. Using ground heat flux, insolation, and latent and sensible heat flux data from the paired sites, IBPM theory's ability to model the oasis effect was analyzed. Wang et al. (2018) define IBPM theory as, "Changes in the surface temperature in response to land use changes are consequences of the local longwave radiative feedback at the surface and energy redistribution brought by changes to the aerodynamic resistance and surface evaporation." In other words, if energy balance is assumed, the temperature difference between two sites is the result of radiative feedback and energy redistribution differences at the sites. This theory has been used to model the effect of afforestation in an arid region of China (Wang et al. (2018)). This study applies IBPM theory to the oasis-desert system. Ground heat flux, the Bowen ratio (the ratio of latent to sensible heat flux) and albedo energy differences are converted to temperature forcings, which are totaled to model the oasis effect. IBPM theory is derived below.

Starting with albedo, the energy forcing due to shortwave radiative feedback can be described by the following equation.

$$\Delta S = (1 - \alpha)K_{\downarrow}$$

where ΔS is the difference in insolation energy between the two sites, K_{\downarrow} is incoming shortwave radiation and α is albedo. K_{\downarrow} is assumed to be equal at the two sites. To calculate convert this energy difference to a temperature forcing, ΔS is multiplied by a linear coefficient.

$$\Delta T_{S_{albedo}} \cong \frac{\lambda_o}{1 + f} \cdot \Delta S$$

where f is the energy redistribution factor and λ_o is the local climate sensitivity. Calculating the energy redistribution factor is beyond the scope of this study. However, a value from the existing literature of 5 (Cao et al., 2016) and a value calculated from MEERA2 Reanalysis of 5.66 for the summer of 2013 (TC Chakraborty, personal communications, 2018) was used in the calculation for arid regions. λ_o is a weak function of temperature and is calculated with the following equation.

$$\lambda_o = \frac{1}{4\sigma T_a^3} = 0.2016 \text{ K W}^{-1}\text{m}^{-2}$$

Ground heat flux is defined as the flow of energy per square meter of soil per second. Its impact on temperature at the two sites is calculated with the following equation.

$$\Delta T_{S_{ground\ heat\ flux}} = \frac{\lambda_o}{1+f} \Delta G$$

where ΔG is the difference in ground heat flux between the two sites.

The final term in IBPM theory involves the Bowen ratio, which is defined as the ratio between sensible and latent heat flux according to the following equation.

$$\beta = \frac{Q_{sensible}}{Q_{latent}}$$

where $Q_{sensible}$ is sensible heat flux and Q_{latent} is latent heat flux. The Bowen ratio is a helpful indicator of how wet an area is. Desert areas have Bowen ratios greater than 10, whereas very wet environments have values of less than 1. The Bowen ratio (average and instantaneous) is used to calculate Δf_2 with the following equation.

$$\Delta T_{S_{Bowen}} \cong \frac{\lambda_o}{(1+f)^2} \cdot \Delta R_n^* \Delta f_2$$

where ΔR_n^* is net apparent radiation and Δf_2 is defined as

$$\Delta f_2 = \frac{\rho_d c_p \lambda_o}{r_T} \left(\frac{\Delta \beta}{\beta^2} \right)$$

where ρ_d is air density, c_p is the specific heat of air, $\Delta \beta$ is the difference in the Bowen ratio between the two sites and β is the average Bowen ratio. r_T is the total heat transfer resistance, which is calculated with the following equation.

$$r_T = \frac{\rho_d c_p \lambda_o}{f} \left(1 + \frac{1}{\beta} \right)$$

Substituting this formula into the Δf_2 equation above, calculation of r_T is avoided. The following equation expresses the difference in energy contribution of latent and sensible heat fluxes.

$$\Delta f_2 = \frac{\Delta \beta f}{\beta^2 \left(1 + \frac{1}{\beta} \right)}$$

This expression can then be rendered into temperature terms in the following equation.

$$\Delta T_{S_{Bowen}} \cong \frac{\lambda_o}{(1+f)^2} \cdot \Delta R_n^* \cdot \frac{\Delta \beta f}{\beta^2 \left(1 + \frac{1}{\beta} \right)}$$

Finally, the total temperature difference can be calculated from the summation of the three components of energy difference between the two sites.

$$\Delta T_s \cong \frac{\lambda_o}{1+f} \cdot \Delta S + \frac{\lambda_o}{(1+f)^2} \cdot \Delta R_n^* \Delta f_2 + \frac{\lambda_o}{1+f} \Delta G$$

where ΔT_s is the difference in surface temperature between the two sites, ΔS is related to the difference in albedo between the two sites, ΔR_n^* is the difference in net radiation between the two sites, Δf_1 is related to the difference in latent heat flux between the sites, and ΔG is the difference in ground heat flux between the two sites.

This theory was applied to the data from 2013 recorded at the desert and oasis field sites. Albedo, α , was calculated as a noontime ratio of average incoming to average outgoing shortwave radiation. The value of f was calculated from a MERRA-2 Reanalysis to be 5.66, the average for summer 2013 (TC Chakraborty, personal communications, 2018). Although the spatial resolution for the MERRA is quite large compared to the distance between the field sites, the results with this f value were comparable to values from the literature (for $f = 4-5$) (Cao et al., 2016 and Bright et al., 2017). λ_o is a weak function of temperature and was calculated with an average summer air temperature of 15 °C.

Ground heat flux, the Bowen ratio, net radiation and insolation were averaged to half-hourly intervals for summer 2013. These values were then entered into the IBPM theory equation, resulting in Figure 12 below. The error in these charts represents on standard deviation of the data, which varied from day to day throughout summer 2013. The Bowen ratio becomes asymptotic when values for latent heat flux are low. Therefore, sensible and latent heat fluxes were averaged to half-hourly intervals for 92 days throughout summer 2013 before values were entered into the IBPM theory equation. Error for the Bowen ratio forcing was calculated based on the three hours before and after noon as an approximation of the range of values for the Bowen ratio during summer 2013.

3.4 Correlation analyses

Correlation analyses were performed to gain insight into the impacts of wind direction, wind speed and atmospheric clarity on the oasis effect. The analysis was thorough but incomplete as there is a wealth of HiWATER data, the analysis of which is beyond the scope of this research project. In the future, it would be useful to incorporate more data from other field sites in the area

and more advanced statistical analyses including multivariate and mixed effects regression models to better understand the relationship between various meteorological variables and the oasis effect.

3.4.1 Wind analysis

Wind speed and direction correlation analyses were performed to empirically understand the relationships between the direction of wind, wind speed and surface and air oasis effects. Wind speed measurements from both the desert and oasis stations were plotted versus surface and air oasis effect to derive empirical linear relationships. Pearson correlation tests were then run on these relationships in order to determine their significance. Wind direction was used stratify the data into two groups: from the northeast (blowing from the oasis towards the desert) and from the southwest (blowing from the desert into the oasis). A P-test was then performed to evaluate whether wind direction had a significant impact on air or surface temperature oasis effects.

3.4.2 Cloudy-day analysis

To understand the impact of cloudy days on the oasis effect, data were stratified into cloudy and sunny days. Following Zhao et al. (2013), the clearness index (k_t) was calculated for each day of summer. k_t is defined by the following equation:

$$k_t = \frac{S}{S_e}$$

where S observed solar radiation and S_e is extraterrestrial radiation at top of atmosphere. S_e is defined by the following equation:

$$S_e = S_{SC} \left[1 + 0.033 \cos \left(\frac{360t_d}{365} \right) \right] \sin \beta$$

where S_{SC} is the solar constant (1.362 kW/m^2), t_d is day of year, and β is solar elevation angle. For Zhangye in summer 2013, S_e is 1360 W m^{-2} , t_d is 182 on July 1 (the mid-point of the observation period) and β is 63 radians (the average for June, July and August at noontime). Converting to degrees, S_e for summer 2013 is calculated to be 1171.8 W m^{-2} .

Days with values of k_t between 0.0 and 0.5 were marked as cloudy, and days with values of k_t between 0.65 and 1.0 were marked as sunny days. The days with values between 0.5 and 0.65 were discarded for this analysis. The surface and air temperature oasis effects on cloudy and sunny days were averaged and a P-test was run to determine whether there was a significant difference between cloudy and sunny day surface and air oasis effects.

4. Results & discussion

4.1 Land use change analysis & remote sensing

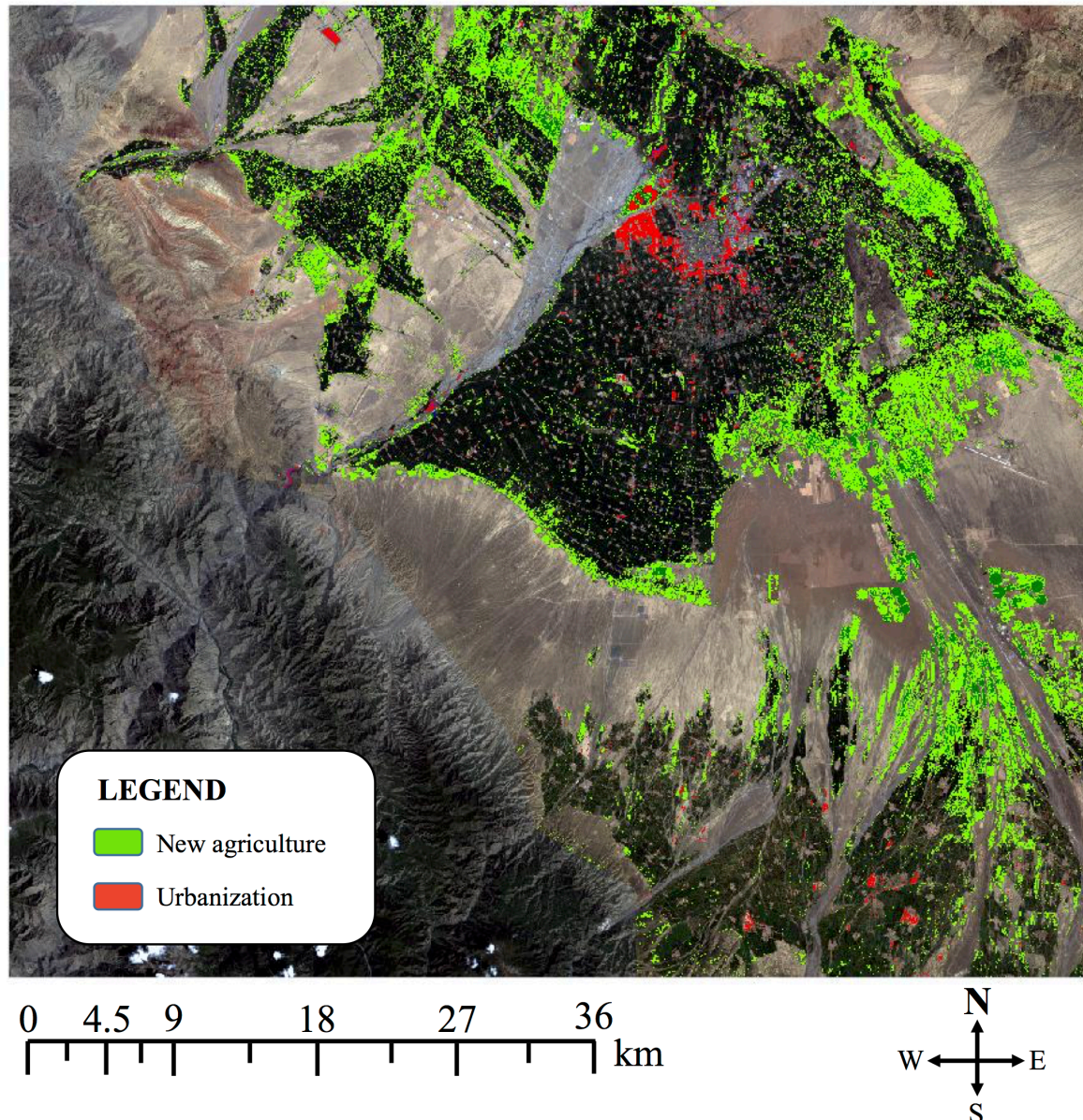


Figure 8: Results of LANDSAT land use change analysis, representing NDVI difference between 1991 to 2013 images. Bright green represents new agriculture (NDVI values of +0.45 to +1.8). Bright red represents new urban areas (NDVI values of -0.22 to -1.58). Note the large expansion of agricultural areas along the desert-oasis interface and in the southeast corner.

As shown in Figure 8 above, between 1991 and 2013, there was a dramatic change in land use around Zhangye. Figure 9 shows the 1991 and 2013 images before ENVI manipulation. Increases in NDVI, corresponding to greening of the land or an increase in agriculture, increased by 4.8%

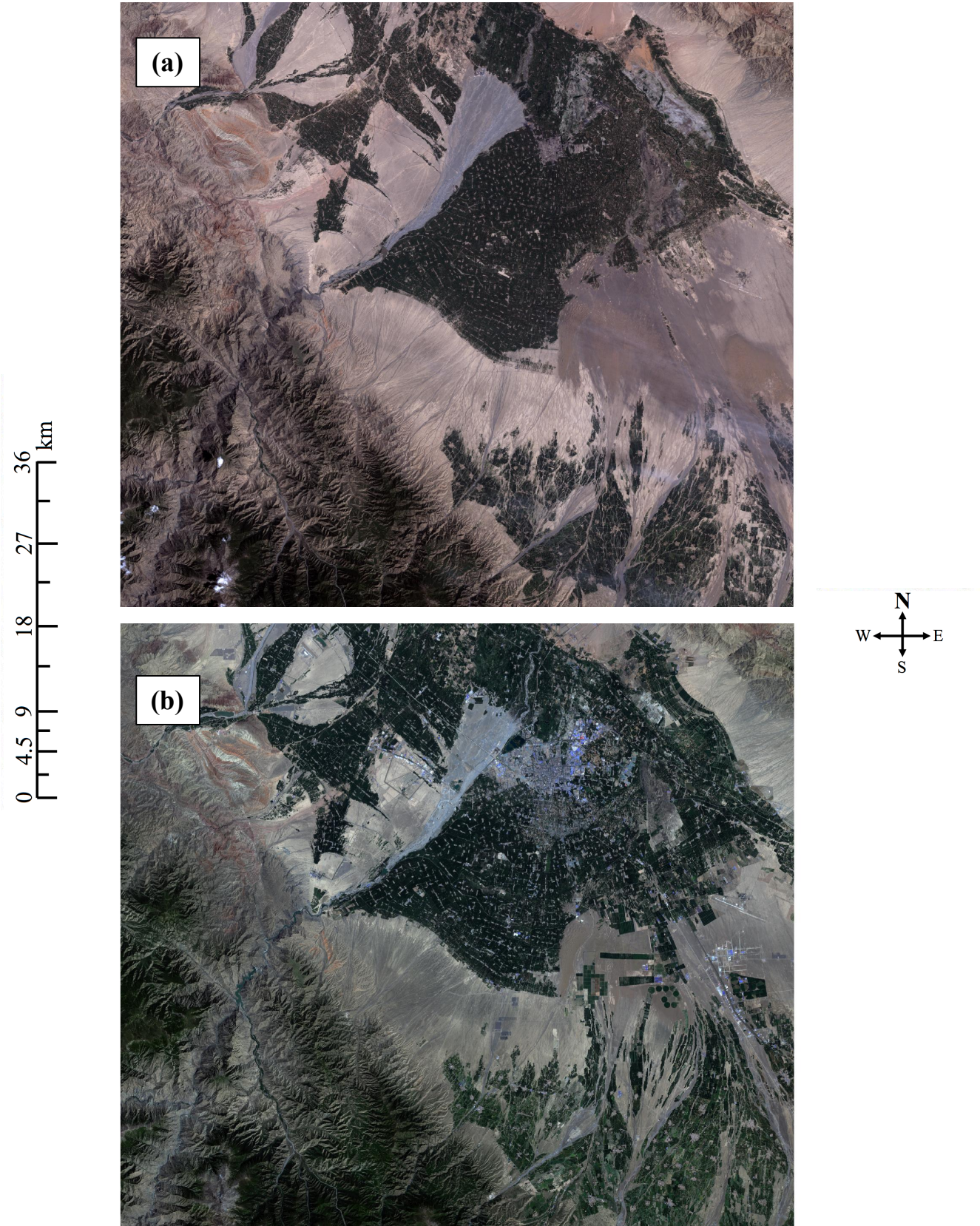


Figure 9: (a) LANDSAT 4-5 432-RGB image from 1991. (b) LANDSAT 8 432-RGB image from 2013. Note the extensive urbanization in Zhangye (center of the scene) and agricultural expansion in the areas outlying the city.

of the scene, or 203.5 km². Between 2002 and 2017, when I visited the area, there had been an even greater expansion of urban and agricultural areas. New urban areas expanded extensively, by 46.7 km² from 1991 to 2013. A larger increase in agriculture between 2002 and 2013 than 1991 and 2002 implies an acceleration in the rate of agricultural expansion in the early 2000s. The decreasing rate of agricultural expansion since 2013 in perhaps due to the increased use of greenhouses, which alter the NDVI values for these areas. Further remote sensing study should investigate the expansion of greenhouse agriculture. The urban land change in 2002-1991 (+1.4) and 2013-2002 (+1.0) do not sum to the 2013-1991 value (+1.1), suggesting that using NDVI and raster slices to track urbanization is not the most accurate assessment. However, it does provide a rough estimate of expanding urban and agricultural areas in Zhangye for the past 20 years. Table 2 shows the changes in land use.

The increase in urban areas and agriculture is related to population growth in the area. During my visit, dozens of new apartment buildings were being constructed at the edges of the city, as well as throughout Gansu Province. The expansion of apartment buildings corresponds to the Chinese government's plans to raise the standard of living for people in the western regions of China. In future studies, a more rigorous quantification method of green house agriculture and urbanization in the area should be applied. For the scope of this study, however, an approximation of total area in land use change shows a general trend of urbanization and expanding agriculture. The values for agricultural expansion can be used to assess the amount of water required to irrigate the new agricultural fields.

Table 2.

Land use change analysis results in area and percentage of total scene by years of study.

Scene difference	Urban land change (km ²)	Urban land change (%)	Agricultural land change (km ²)	Agricultural land change (%)
2002 – 1991	+57.6	+1.4	+20.5	+0.5
2013 – 2002	+41.5	+1.0	+107.1	+2.5
2013 – 1991	+46.7	+1.1	+203.5	+4.8
2017 – 2013	+87.9	+2.1	+45.7	+1.1
2017 – 1990	+65.6	+1.5	+296.9	+7.0

As discussed above, 600 mm is a conservative estimate for seasonal evapotranspiration in the Heihe River Basin's agricultural areas (Liang & Huang, 2015). Using this estimate, the total

amount of increased water demand can be calculated. Zhang et al. (2015) showed an average streamflow from 1945 to 2012 at an upstream station (before the Heihe River reaches agricultural areas in Zhangye) of $15.84 \times 10^8 \text{ m}^3$. The average streamflow from 1977 to 2010 at a downstream station (past the agricultural areas in Zhangye) was $10.34 \times 10^8 \text{ m}^3$, suggesting a total of $5.5 \times 10^8 \text{ m}^3$ was removed from the Heihe River for irrigated agriculture. The amount of water required for the new irrigated lands quantified in the remote sensing analysis was compared to these values with the following equation.

$$V_{required} = ET_{seasonal} * A$$

where $V_{required}$ is the volume of water demand for seasonal agricultural irrigation (m^3), $ET_{seasonal}$ is the seasonal evapotranspiration of irrigated fields, and A is the area of new agriculture. Table 3 shows the results of this calculation. The water required for the expanded agricultural areas from 1991 to 2017 increased by $17.81 \times 10^7 \text{ m}^3$, or 11.25% of the historical average upstream flow. These results suggest a large increase in water consumption associated with expanding agriculture in the past 20 years. This increase corresponds to significant increasing demands on water resources in Zhangye, Gansu, China, despite the recent attempts to limit water usage. However, these results may need adjustment in future studies, as water-saving technologies including drip-irrigation have been increasingly implemented in Zhangye, limiting the water demands in agricultural fields.

Table 3.

Results of the water demand calculation, with volume of required water and its percentage of upstream flow.

Scene difference	$V_{required} (10^7 \text{ m}^3)$	% of average upstream flow
2002 – 1991	1.23	0.78
2013 – 2002	6.42	4.06
2013 – 1991	12.21	7.71
2017 – 2013	2.74	1.73
2017 – 1991	17.81	11.25

4.2 A statistical depiction of the oasis effect

The oasis effect was observed at the desert and oasis stations during the summer of 2013. Figure 10 shows the seasonal hourly averages and standard deviation of surface and air temperature oasis effects. In summer at 14:00 the surface oasis effect is the most pronounced. In other words, the difference in surface temperature between the oasis and desert field sites is largest during

summer afternoon, with surface temperature oasis effect values reaching $-12\text{ }^{\circ}\text{C}$ on average. This trend is due to the fact that insolation is most intense during summer months at noontime. The delay in peak oasis effect is likely due to a lag time in energy redistribution. The surface oasis

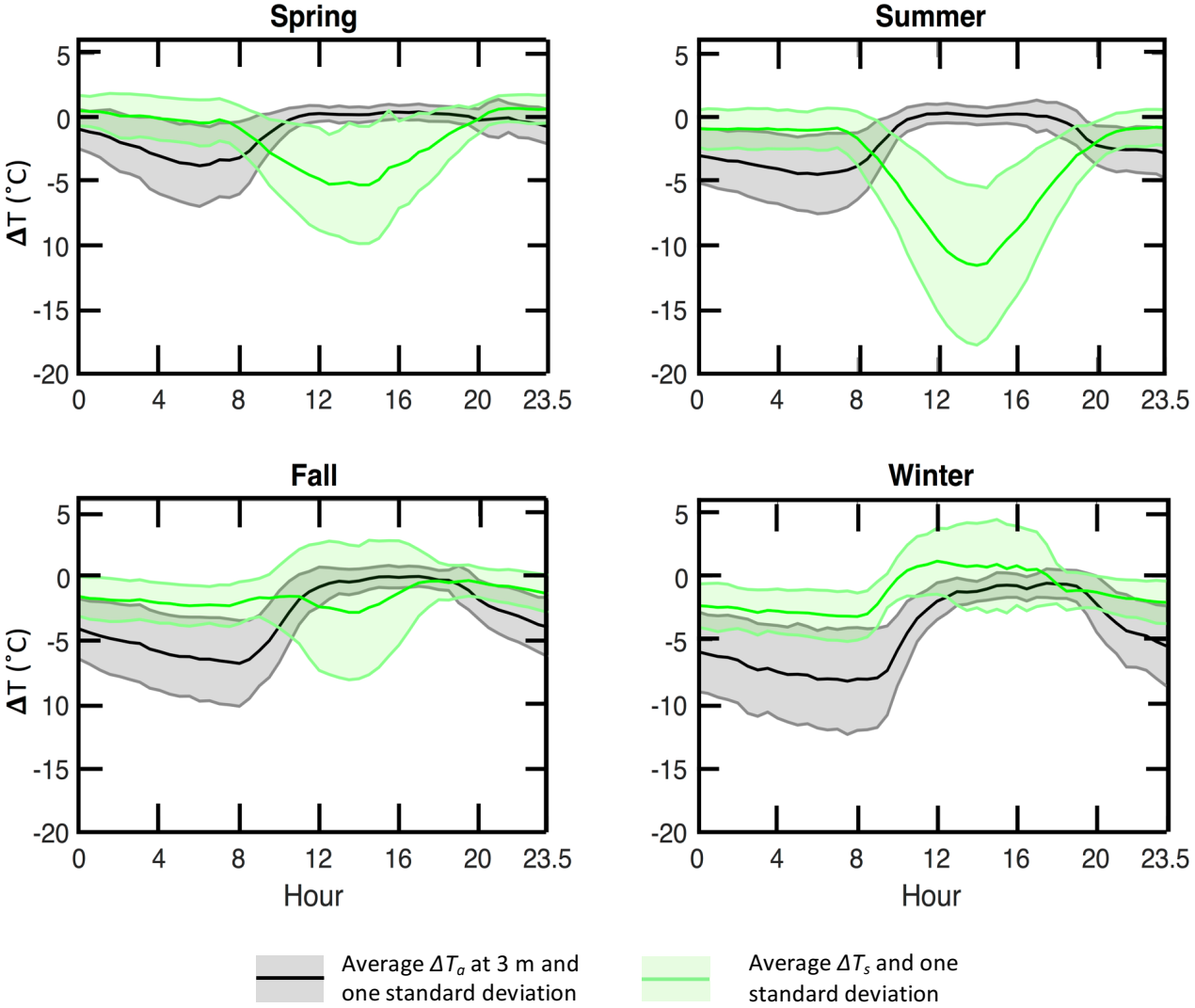


Figure 10: Average hourly oasis effect in four seasons. Solid green line and green shading represent mean surface temperature oasis effect and one standard deviation. Solid black line and grey shading represent mean air temperature oasis effect and one standard deviation. Note the large surface temperature oasis effect in summer at 14:00.

effect is somewhat prominent in spring time, with an average peak effect of about $-5\text{ }^{\circ}\text{C}$ at 14:00. The surface oasis effect is less extreme but still statistically distinct in the fall at 14:00 with average effect values of $-2\text{ }^{\circ}\text{C}$. In spring, fall and summer, the surface oasis effect is close to $0\text{ }^{\circ}\text{C}$ throughout the night. In winter, this effect is reversed the surface oasis effect is almost $0\text{ }^{\circ}\text{C}$ average at noontime

and approximately -3°C average during the night. This trend is perhaps due to changes in albedo, precipitation and vegetation cover throughout the year.

The air oasis effect, taken as the difference in air temperature at 3 m between the two sites, shows a statistically distinct seasonal and hourly pattern. In all seasons, noontime air temperature oasis effect values are approximately 0°C . At nighttime, however, air temperature oasis effects are consistently more prominent, with average values ranging from -4°C , -5°C , -7°C and -8°C , for spring, summer, fall and winter respectively.

Generally, the surface oasis effect is greatest in summer during the afternoon. For this study, IBPM theory was applied only to noontime in the summer. Noontime was chosen due to the fact that albedo calculations become asymptotic as the sun's zenith angle decreases. However, in future studies, applying IBPM theory at hourly intervals (especially at 14:00) and throughout the year would be helpful in providing a mechanistic understanding of the observed patterns in surface and air temperature oasis effects.

4.3 IBPM theory results

IBPM theory was shown to successfully model the oasis effect at noon and midnight during summer of 2013. The following section discusses individual energy forcings as well as the final result of IBPM theory. Table 4 shows intermediate values before the terms were multiplied by the coefficient to convert these from energy forcings (in W m^{-2}) to temperature ($^{\circ}\text{C}$). This table shows that the temperature forcings are much smaller in magnitude at night due to the fact that less energy enters the system without insolation. Figure 12, below, shows a scatter plot of temperature forcings versus the observed oasis effect for individual days of summer.

Albedo was calculated throughout the year as the ratio between average incoming and outgoing shortwave radiation. Figure 11 shows the values of albedo for each season at both the desert and oasis sites. Winter had the lowest albedo values for both the desert and oasis sites. This is due to the fact that there is little vegetation in the winter, resulting in brighter land surfaces. The summer had the lowest albedo for both sites, due to increased vegetation and a darker land cover. In all cases, the oasis had a larger albedo than the desert, implying that the oasis absorbs more shortwave insolation than the desert site. This result would suggest that the oasis should be warmer than the desert, resulting in a positive oasis effect. However, this forcing is smaller in magnitude than the Bowen ratio forcing, which is negative, resulting in the observed negative surface temperature oasis effect.

Table 4.

Intermediate forcing values of IBPM theory. These values correspond to average summer energy differences between the two sites before multiplication by a coefficient.

Hour	Forcing (W m^{-2})		
	ΔS	$\Delta\beta$	ΔG
Noon	59.290	-0.703	-15.709
Midnight	0.001	-0.147	4.063

The Bowen ratio, which is defined as the ratio between sensible and latent heat flux, had the largest impact on the oasis effect in summer. In agreement with Kai et al. (1997) and Hao et al. (2016), the oasis effect largely results from significant upward latent heat flux over the oasis due to evaporation. At noontime, the positive forcing of albedo ($+2.4^\circ\text{C}$ on average) is balanced by the large average Bowen ratio forcing (-9.6°C on average). Ground heat flux contributes a small

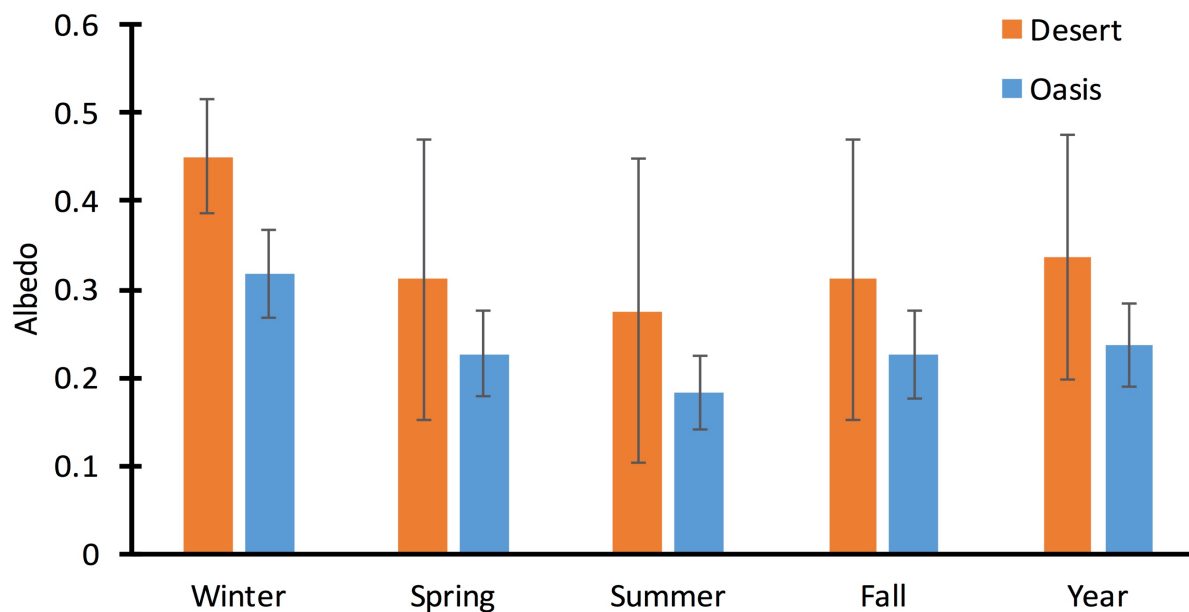


Figure 11: Average noontime albedo and standard deviation for spring, summer, fall, winter and yearly average albedo and standard deviation. The desert site (orange) has a higher albedo throughout the year. The oasis site (blue) has a lower albedo throughout the year. For both sites, albedo is highest in the winter due to lack of vegetation and lowest in the summer due to vegetation.

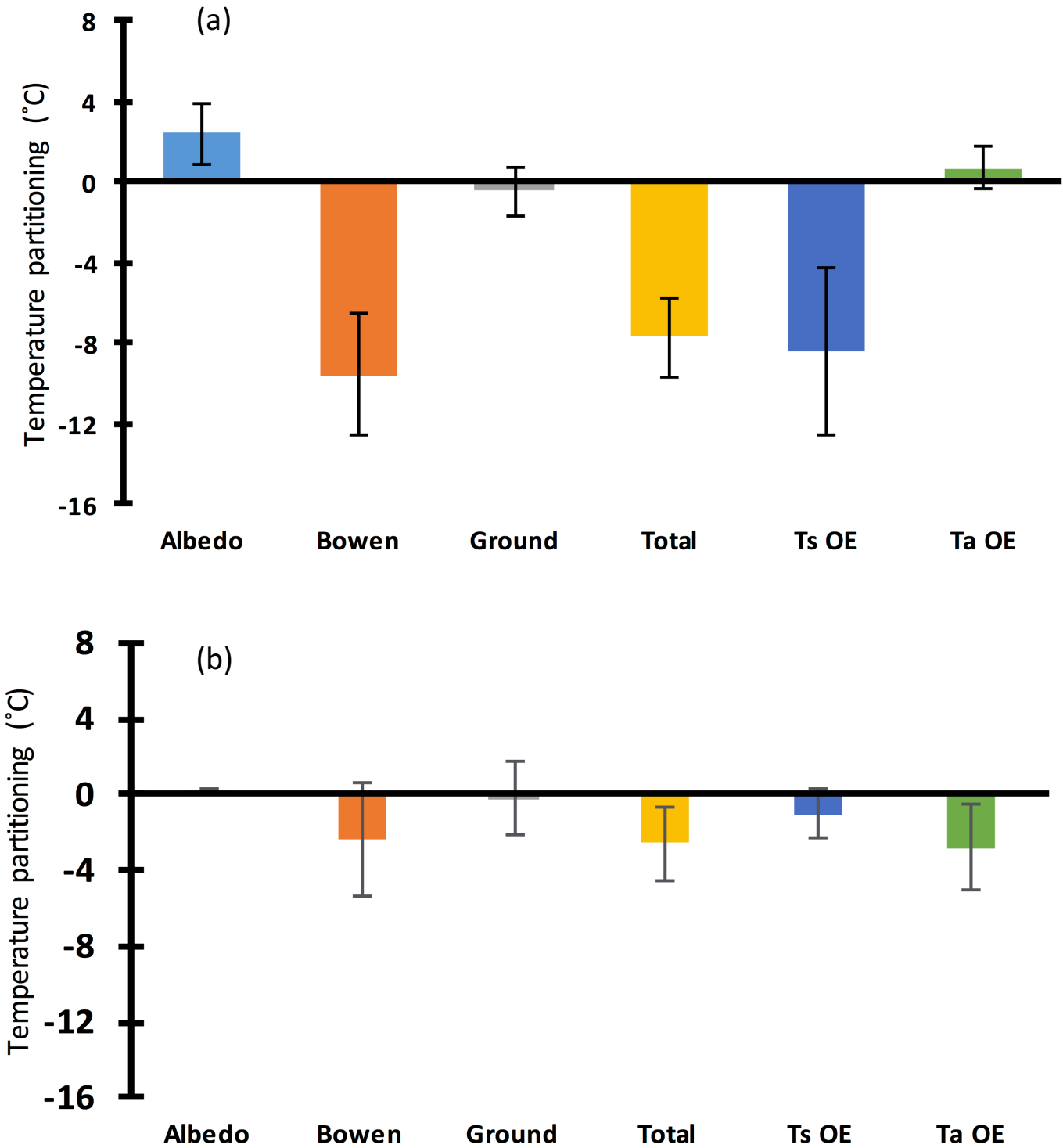


Figure 12: IBPM theory applied at (a) noontime and (b) midnight in summer 2013 successfully predicts the surface temperature oasis effect. Albedo (light blue), Bowen ratio (orange), and ground heat flux (grey) terms are summed to the total (yellow), which closely approximates the observed surface oasis effect (Ts OE, in dark blue) in magnitude and sign. Surface temperature oasis effect (Ta OE, in green) is also shown.

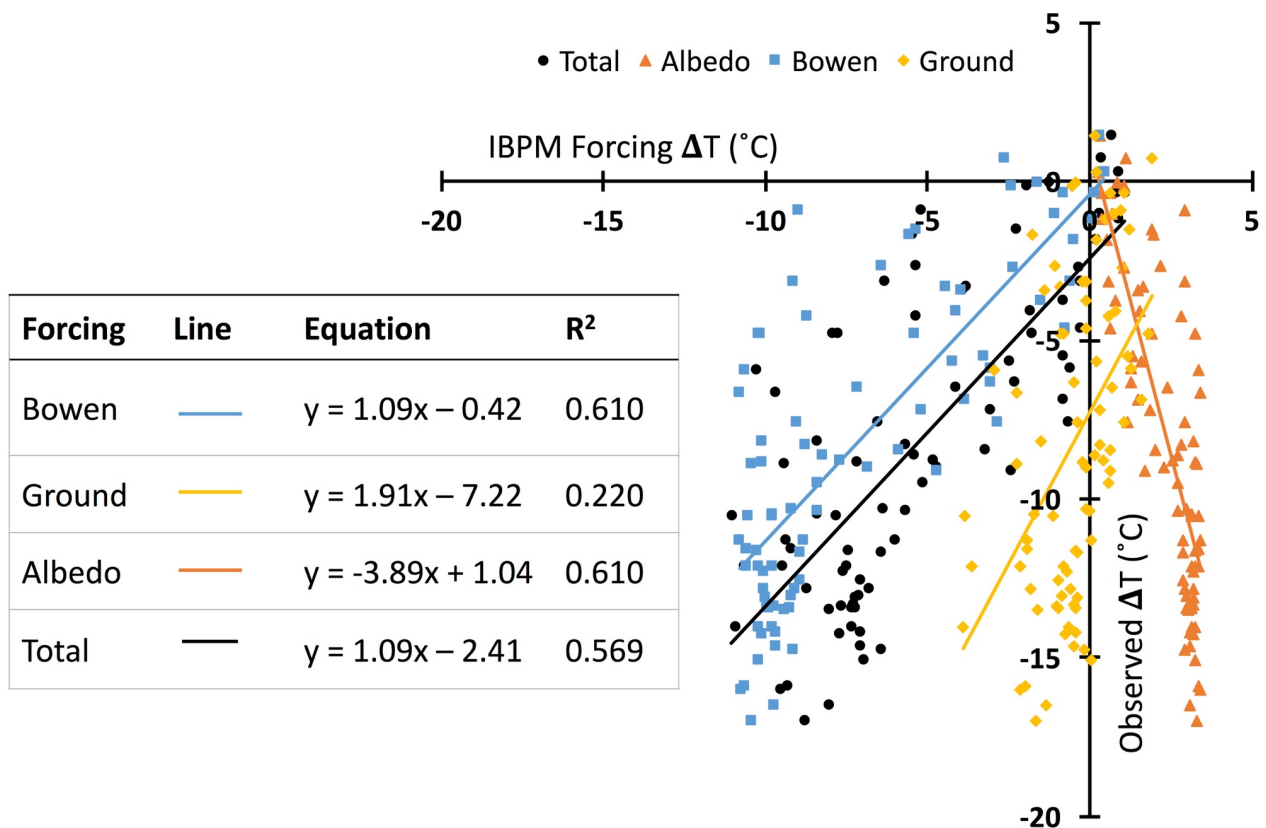


Figure 13: Scatter plot of individual noontime IBPM forcings and total predicted surface oasis effect versus observed surface oasis effect. The table shows the empirically-derived linear relationships between surface oasis effect and the individual forcing terms. The Bowen ratio most closely approximates the observed oasis effect in slope and intercept.

average negative forcing (-0.5°C). Summing these three temperature forcing values (albedo, Bowen ratio and ground heat flux), the predicted oasis effect from IBPM theory (-7.7°C) closely approximates the observed average surface temperature oasis effect (-8.4°C) in summer 2013. Figure 13 shows a scatter plot of individual forcings at noon and midnight for the 92 days that consisted of the 2013 summer dataset. The empirical relationships between the observed surface temperature oasis effect is plotted against the individual forcings in IBPM theory and total predicted oasis effect. Albedo and the Bowen ratio are more closely correlated to the observed oasis effect (with R^2 values of 0.61), whereas ground heat flux has a more scattered relationship to the observed oasis effect (with an R^2 value of 0.22). The Bowen ratio is the dominating effect, with an equivalent slope to the total predicted oasis effect. The slope of the albedo forcing relationship is about 3.9 times larger than the slope of the predicted total effect. This value suggests the relationship is nonlinear. Figure 14 shows a rank analysis of the observed surface temperature

oasis effect and the albedo forcing rank. This relationship is closer to a 1:1 line with a slope of approximately -0.72, showing a parametric relationship between albedo temperature forcing and the surface temperature oasis effect exists. This is likely due to insolation variation, which is discussed in detail below in the insolation correlation analysis. In future studies, stratifying the data into cloudy and sunny days would decrease the scatter between IBPM theory's predicted oasis effect and the observed surface temperature oasis effect.

IBPM theory can successfully model the oasis effect at summer noontime based on three energy forcings: albedo (related to insolation), ground heat flux, and the Bowen ratio (related to latent heat flux). This mechanistic approach is helpful in understanding how and when the oasis effect arises. From this analysis, latent heat flux emerges as the forcing that most strongly determines the oasis effect, suggesting that water is important not only for agriculture, but also for maintaining a cool climate in the oasis.

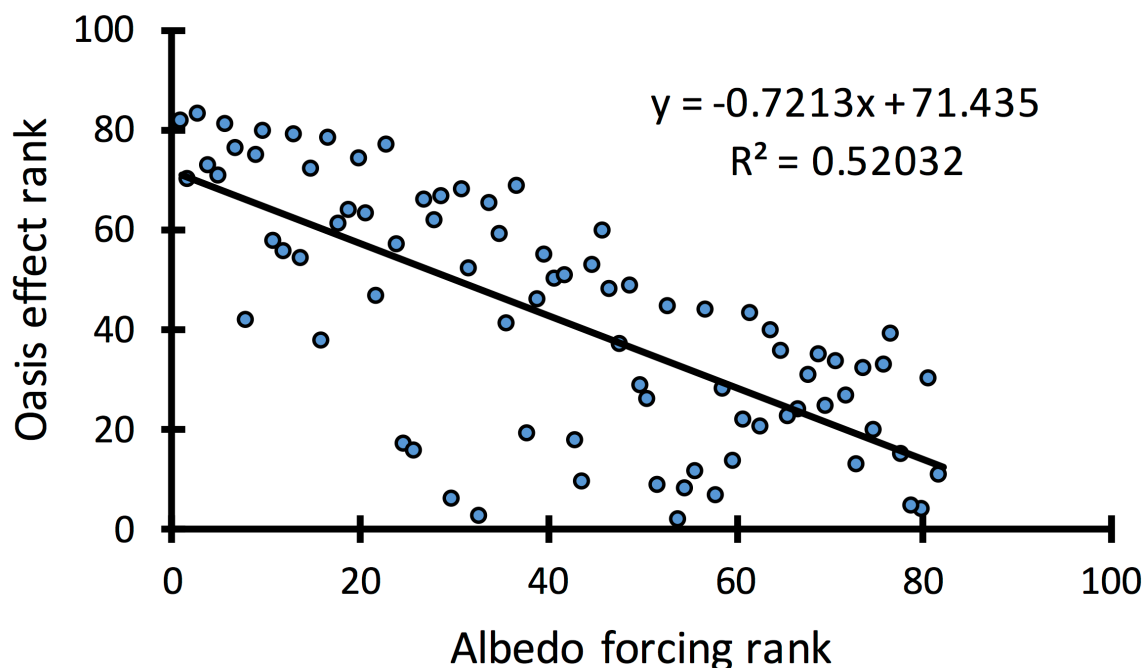


Figure 14: Albedo forcing rank vs. surface temperature oasis effect rank. This simple rank analysis helps remove the nonlinearity in the data, revealing a remarkably linear relationship between the oasis effect and albedo forcing ranks.

4.4 Correlation analyses results

These correlation results are helpful in understanding the dynamics of variables that control the magnitude of the oasis effect in summer 2013. Air temperature and surface temperature oasis

effects show strikingly different patterns throughout the year, as discussed above. The results of this study show that insolation is closely related to surface temperature oasis effect. Wind speed also has a significant but scattered impact on the air temperature oasis effect. Wind direction has some impact, but further study is required to fully appreciate the mechanisms by which wind direction affects oasis effects in Zhangye.

4.4.1 Wind speed and direction

The results of the wind analysis show that wind speed has a significant but scattered impact on air temperature oasis effects at noontime. Wind direction has a limited impact on the oasis effect; however, this result is likely due to the system's complexity. Future studies should incorporate more data from several different field sites to investigate the dynamics of wind direction and oasis effects. Literature on this topic has drawn mixed conclusions. Porcheter et al. (2008) and Taha et al. (1991) showed that increased wind speed correlated to a decreased oasis effect, whereas Kai et al.'s (1997) results show a correlation between wind speed and an increase oasis effect due to increased sensible heat flux over the desert.

Table 5.

The results of wind speed correlation analysis.

Hour	Site	Oasis effect (ΔT)	Linear equation (y is oasis effect in $^{\circ}\text{C}$ and x is wind speed in m s^{-2})	R^2	P-value
12:00	Desert	Surface	$y = -0.33x - 7.51$	0.0084	0.386
		Air	$y = -0.19x + 0.88$	0.129	0.00043
	Oasis	Surface	$y = -0.58x - 9.4$	0.012	0.306
		Air	$y = -0.19x + 0.62$	0.054	0.0258
0:00	Desert	Surface	$y = -0.07x - 0.6$	0.0079	0.398
		Air	$y = -0.18x - 2.3$	0.0244	0.137
	Oasis	Surface	$y = 0.45x - 1.36$	0.103	0.0018
		Air	$y = 0.78x - 3.8$	0.144	0.00019

The results of the wind speed analysis show that there are significant linear relationships between noon desert wind speed and air temperature oasis effect, noon oasis wind speed and air temperature oasis effect, and midnight oasis wind speed and surface and air oasis effects. Higher wind speed is correlated to increases in air temperature oasis effect at noon. For the oasis site at

midnight, there is a significant relationship between air speed and the surface and air temperature oasis effects. Table 5 above summarizes the results of the wind speed analysis. Figure 15 shows the results of the wind direction analysis.

The P-values in Table 5 demonstrate a significant relationship between air temperature oasis effect and wind speed measured over the desert station, implying a negative relationship between desert wind speed and oasis effect, or increased air temperature oasis effect with windier conditions. Likewise, the air temperature oasis effect is stronger with higher winds over the desert.

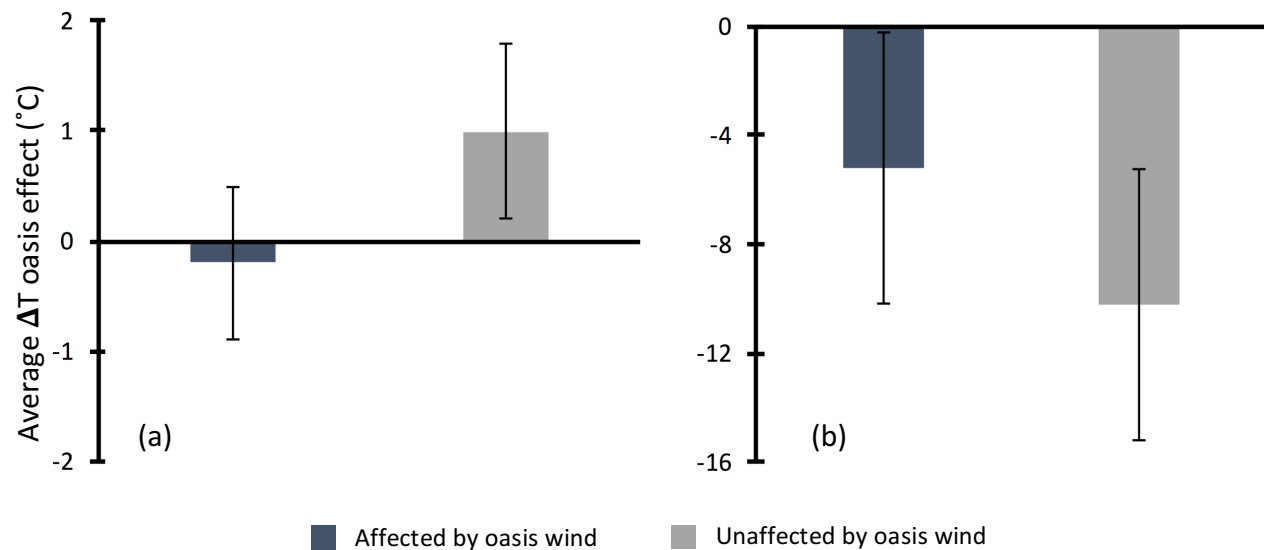


Figure 15: Results of wind direction correlation analysis. (a) Impact of wind direction on air temperature oasis effect. (b) Impact of wind direction on surface temperature oasis effect. Data were stratified depending on wind direction. 'Affected by oasis wind' signifies that the wind was blowing from the northeast, from the oasis into the desert. 'Unaffected by oasis wind' signifies that wind direction was from the southwest, from the desert towards the oasis.

These results confirm the findings of Kai et al. (1997) and refute the findings of Porcheter et al. (2008) and Taha et al. (1991), implying that sensible heat flux over the oasis may increase with wind speed and therefore magnify the air temperature oasis effect. Furthermore, a significant positive relationship appears at midnight at the oasis station for both surface and air temperature oasis effects, implying that less wind at the oasis at midnight results in larger oasis effect. These mixed results are due to the fact that this system is more complicated than these measurements are able to reveal. Furthermore, the R^2 values are small for each of these relationships, suggesting that wind speed has weak correlation with oasis effects. Due to the scattered correlation, however,

IBPM analysis above can be performed without stratifying the data into windy and non-windy days.

Wind direction correlation analysis reveals that when the wind blows from the northwest (affected by the oasis), air temperature oasis effect decreases. When wind blows from the southwest, air temperature oasis effect increases but surface temperature oasis effect decreases. Both of these results are significant (P-values of 0.003 and 0.00016 for T_a and T_s oasis effects, respectively). The results for air temperature oasis effect are unexpected. With air blowing from the desert towards the oasis, the desert temperatures are expected to be unaffected by the cool oasis, and therefore be warmer (resulting in a greater oasis effect). However, the air temperature oasis effect is smaller with desert air unaffected by the cool oasis. This result may arise from the fact that the system is more complicated than can be resolved by only two data sets. The results of

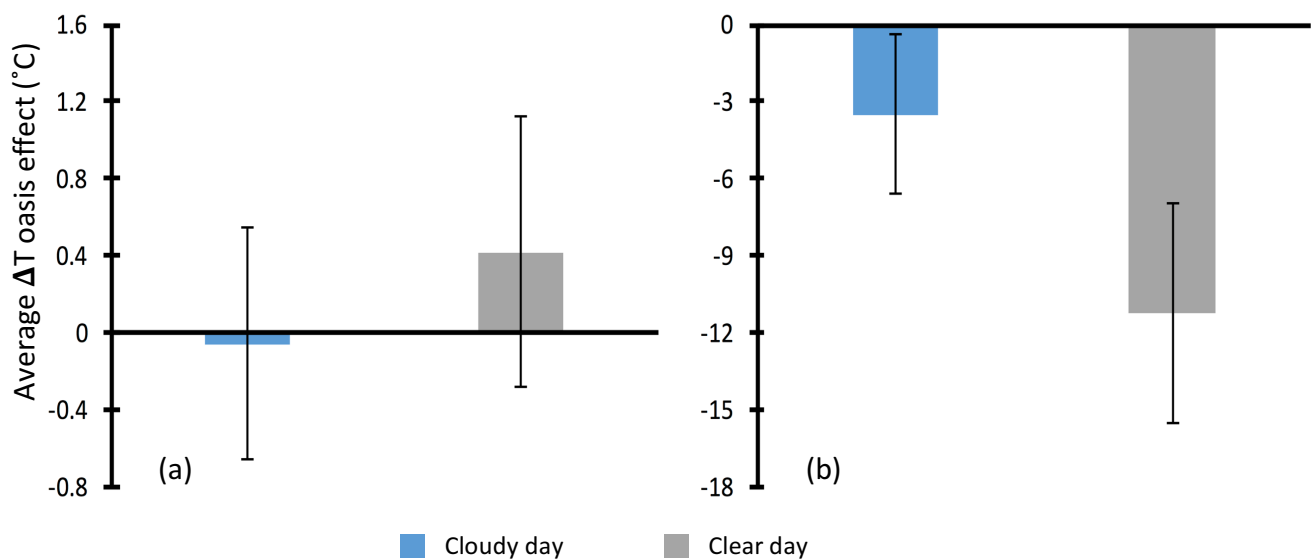


Figure 16: Results of insolation correlation analysis for (a) air temperature and (b) surface temperature oasis effects. Cloudy days are defined with k_t values of 0.0-0.5. Clear days are defined with k_t values of 0.65-1.0. As expected, a larger surface temperature oasis effect is observed on sunny days when there is more intense latent heat flux due to increased evaporation. Insolation has a less dramatic impact on air temperature oasis effect, but reveals an opposite trend, with clear days resulting in decreased oasis effect.

the surface temperature oasis effect are as expected. A greater surface temperature oasis effect is observed when the desert station is unaffected by wind blowing from the cool oasis.

Wind speed and direction correlation analyses showed that wind speed increased air temperature oasis effects. Because of the insignificant correlation between wind speed and surface

temperature oasis effect during noontime, IBPM theory can be applied without stratifying data into windy/calm days. However, wind direction did have a significant impact on surface temperature oasis effect, suggesting that future studies should stratify data depending on wind direction to improve IBPM theory's ability to model the oasis effect.

4.4.2 Cloudy-day analysis results

Insolation correlation analysis was performed to investigate the impact of atmospheric clarity on surface and air temperature oasis effect. This analysis is useful in better understanding the statistical depiction of air and surface temperature oasis effects discussed above. As Figure 16, above, shows, there is a significant relationship between cloudy days and clear days. During sunny days, there is an increase in incoming insolation, resulting in more evaporation over the oasis. This results in significantly larger surface temperature oasis effects at noontime. This result supports the conclusion of IBPM theory that latent heat flux is the dominant term controlling the oasis effect. The opposite trend occurs for air temperature oasis effect, with more insolation resulting in less of an oasis effect. Both of these relationships are significant (with p-values of 0.0041 and 4.1E-12 for T_a and T_s respectively).

5. Conclusion

This study investigates the oasis effect in Zhangye, Gansu, China, with the goals of better understanding local water demand and land use change, developing a statistical understanding of the oasis effect, evaluating the ability of IBPM theory to predict the oasis effect, and performing a correlation analysis of insolation and wind variables to predict their impacts on oasis effects. Land use change analysis revealed a positive trend in urbanization and rapid increase in agricultural areas, resulting in an increase of 11.25% in water demand in the past 26 years alone. This result is consistent with recent literature, which suggests a continued increase in water demand due to population growth and economic development. The analysis of the data from HiWATER shows that an oasis effect was observed between the desert and oasis sites for the summer of 2013. The effect was greatest during the summer months during the afternoon. Air temperature oasis effect shows the opposite trend throughout the year, with a greater oasis effect during nighttime hours. The results of this statistical analysis confirm the findings of previous studies of the oasis effect, which argue that the oasis effect occurs due to intense latent heat flux over the oasis. IBPM theory

can successfully be applied to an oasis-desert system as it accurately predicts the sign and magnitude of the oasis effect during the summer months at noon and midnight. This mechanistic understanding of the oasis effect is useful in predicting surface temperature oasis effect and could be applied in future studies to estimate the amount of water required to produce a desired oasis effect. Correlation analyses between wind speed and surface and air temperature oasis effects showed a significant empirical relationship between wind speed and air temperature oasis effect, confirming the finding by Kai et al. (1997) that sensible heat flux over the oasis increases on windy days, increasing the air temperature oasis effect. An unexpected relationship between wind direction and air temperature oasis effect was found, showing that the oasis effect increased when oasis wind contaminated the air at the desert station. However, the system is more complex than the scope of this study, resulting in confounded results. Wind direction impacted surface temperature oasis effects when blowing from the oasis into the desert (cooling the desert station and decreasing the oasis effect). Insolation was shown to have a significant impact on surface oasis effect, confirming the theory that latent heat flux controls the surface temperature oasis effect via evaporation.

Remote sensing analysis should be refined in future research. As urban areas were unsuccessfully resolved and greenhouse agriculture is increasing in Zhangye, a more precise method of quantifying land use change would be useful in approximating water consumption in Zhangye. Applying IBPM theory at hourly intervals in for each season could prove helpful in further developing a mechanistic understanding of the oasis effect and what temperature forcings have the largest impact on the oasis effect. Further research is also required into the impacts of wind and circulation over the system and their implications for the oasis effect.

Ultimately, this study provides insight into the the local context of agriculture in Zhangye and the study of the oasis effect there. Oasis agriculture around the world is threatened by climate change and unsustainable water usage. IBPM theory, remote sensing and correlation analysis prove to be useful tools in researching the hydrology of these regions, with the goal of sustainable water management. As Hao et al. (2016) show, the oasis effect is diminishing in northwest China, leading to faster rates of warming than the rest of the country. As this study shows, the oasis effect arises largely from latent heat flux. Water is not only essential to life as well as agricultural and economy activity in arid regions; it also plays a large role in regional climate dynamics. With

continuing research in this field, balancing the needs of industry, agriculture and the environment as well as predicting future needs can be met.

Acknowledgements

I have deeply appreciated the opportunity to work with Professor Xuhui Lee. His patience, generosity and mentorship made me feel ready to take on this project. Professor Lee has also shown me how fun and engaging research can be, and I am very grateful for his guidance and support throughout this year. I am also thankful for Professor Ron Smith and Professor Mary Louise Timmermans and their continued support, both throughout this year and previous. Thank you to Larry Bonneau, who was always welcoming and kind, even in my last-minute pursuits of remote sensing data. I am also very grateful to the members of Professor Lee's lab, including Bowen Fang, Natalie Schultz and TC Chakraborty, who provided thoughtful insight about my research and support during my travels. With funding from the Karen Von Damm '84 Fellowship, I was able to visit my study site in Zhangye and present my research to colleagues at the Beijing Normal University and in Lanzhou. In China, I was welcomed with incredible hospitality by Professor Ziwei Zu, Professor Xiaofan Yang, Professor Xin Li, and graduate students Yanzhao Zhou, Xiang Li, Xiaochen Wang, Lu Zheng and Jun. I would also like to thank Professor Michael M. Dove for his advice on the sociopolitical aspects of my thesis and proposal-writing, as well as his encouragement and patience. Professor David Evans, Professor Jay Ague and Professor Alexey Fedorov have made the G&G major exciting and challenging for me, and I thank them for their inspired teaching.

My New Haven family, including Sophie Freeman, Alex Saiontz, Rohan Naik, Maya Jenkins, Annie Nelson, Dimitri Diagne, Michelle Liu, John Lee, Julia Hamer-Light, Athena Wheaton, Julia Rosenheim, and the members of Looking Glass 2018, was integral in the completion of this project and my senior year. A huge and loving thank you to my parents, for their care and support, no matter how far away my adventures may take me.

Bibliography

- Bjurström, A., & Polk, M. (2011). Physical and economic bias in climate change research: a scientometric study of IPCC Third Assessment Report. *Climate Change*, 108(1–2), 1–22. <https://doi.org/10.1007/s10584-011-0018-8>
- Bright, R. M., Davin, E., O'Halloran, T., Pongratz, J., Zhao, K., & Cescatti, A. (2017). Local temperature response to land cover and management change driven by non-radiative processes. *Nature Climate Change*, 7(4), 296. <https://doi.org/10.1038/nclimate3250>
- Cao, C., Lee, X., Liu, S., Schultz, N., Xiao, W., Zhang, M., & Zhao, L. (2016). Urban heat islands in China enhanced by haze pollution. *Nature Communications*, 7, 12509. <https://doi.org/10.1038/ncomms12509>
- Chen, Y., Zhang, D., Sun, Y., Liu, X., Wang, N., & Savenije, H. H. G. (2005). Water demand management: A case study of the Heihe River Basin in China. *Physics and Chemistry of the Earth*, 30(6–7), 408–419. <https://doi.org/10.1016/j.pce.2005.06.019>

- Cheng, G., Li, X., Zhao, W., Xu, Z., Feng, Q., Xiao, S., & Xiao, H. (2014). Integrated study of the water–ecosystem–economy in the Heihe River Basin. *National Science Review*, 1(3), 413–428. <https://doi.org/10.1093/nsr/nwu017>
- Chu, P., Lyu, S., & Chen, Y. (2005). A numerical modeling study on desert oasis self-supporting mechanisms. *Journal of Hydrology*, 312, 256–276. <https://doi.org/10.1016/j.jhydrol.2005.02.043>
- Hao, X., Li, W., & Deng, H. (2016). The oasis effect and summer temperature rise in arid regions - Case study in Tarim Basin. *Scientific Reports*, 6, 35418. <https://doi.org/10.1038/srep35418>
- Huang, C., Chen, W., Li, Y., Shen, H., & Li, X. (2016). Assimilating multi-source data into land surface model to simultaneously improve estimations of soil moisture, soil temperature, and surface turbulent fluxes in irrigated fields. *Agricultural and Forest Meteorology*, 230–231, 142–156. <https://doi.org/10.1016/j.agrformet.2016.03.013>
- Huang, G., Li, X., Ma, M., Li, H., & Huang, C. (2016). High resolution surface radiation products for studies of regional energy, hydrologic and ecological processes over Heihe river basin, northwest China. *Agricultural and Forest Meteorology*, 230–231, 67–78. <https://doi.org/10.1016/j.agrformet.2016.04.007>
- Jinjiao, L., & Huang, M. (2015). Evapotranspiration Estimation for an Oasis Area in the Heihe River Basin Using Landsat-8 Images and the METRIC Model. *Water Resources Management*, 29. <https://doi.org/10.1007/s11269-015-1110-z>
- Kai, K., Matsuda, M., & Sato, R. (1997). Oasis Effect Observed at Zhangye Oasis in the Hexi Corridor, China. *Journal of the Meteorological Society of Japan*, 75(6), 1171–1178.
- Lee, X. (2018). *Fundamentals of Boundary-Layer Meteorology*. Springer International Publishing. Retrieved from [//www.springer.com/de/book/9783319608518](http://www.springer.com/de/book/9783319608518)
- Lee, X., Goulden, M. L., Hollinger, D. Y., Barr, A., Black, T. A., Bohrer, G., ... Zhao, L. (2011). Observed increase in local cooling effect of deforestation at higher latitudes. *Nature*, 479(7373), 384–387. <https://doi.org/10.1038/nature10588>
- Li, X., Cheng, G., Liu, S., Xiao, Q., Ma, M., Jin, R., ... Xu, Z. (2013). Heihe Watershed Allied Telemetry Experimental Research (HiWATER): Scientific Objectives and Experimental Design. *Bulletin of the American Meteorological Society*, 94(8), 1145–1160. <https://doi.org/10.1175/BAMS-D-12-00154.1>
- Li, X., Liu, S., Xiao, Q., Ma, M., Jin, R., Che, T., ... Wang, L. (2017). A multiscale dataset for understanding complex eco-hydrological processes in a heterogeneous oasis system. *Scientific Data*, 4, 170083. <https://doi.org/10.1038/sdata.2017.83>
- Li, X., Yang, K., & Zhou, Y. (2016). Progress in the study of oasis-desert interactions. *Agricultural and Forest Meteorology*, 230–231, 1–7. <https://doi.org/10.1016/j.agrformet.2016.08.022>
- Li Xin, Cheng Guodong, Ge Yingchun, Li Hongyi, Han Feng, Hu Xiaoli, ... Cai Ximing. (2018). Hydrological Cycle in the Heihe River Basin and Its Implication for Water Resource Management in Endorheic Basins. *Journal of Geophysical Research: Atmospheres*, 123(2), 890–914. <https://doi.org/10.1002/2017JD027889>
- Liu, S. M., Xu, Z. W., Wang, W. Z., Jia, Z. Z., Zhu, M. J., Bai, J., & Wang, J. M. (2011). A comparison of eddy-covariance and large aperture scintillometer measurements with respect to the energy balance closure problem. *Hydrol. Earth Syst. Sci.*, 15(4), 1291–1306. <https://doi.org/10.5194/hess-15-1291-2011>

- Meng, W. (2009). *The Water Cries*. Asia Pacific Films. Retrieved from http://www.cctv.com/program/e_documentary/20090430/101130.shtml
- Micklin, P. P. (1988). Desiccation of the aral sea: a water management disaster in the soviet union. *Science (New York, N.Y.)*, 241(4870), 1170–1176. <https://doi.org/10.1126/science.241.4870.1170>
- Peng, H., Cheng, G., Xu, Z., Yin, Y., & Xu, W. (2007). Social, economic, and ecological impacts of the “Grain for Green” project in China: A preliminary case in Zhangye, Northwest China. *Journal of Environmental Management*, 85(3), 774–784. <https://doi.org/10.1016/j.jenvman.2006.09.015>
- Potchter, O., Goldman, D., Kadish, D., & Iluz, D. (2008). The oasis effect in an extremely hot and arid climate: The case of southern Israel. *Journal of Arid Environments*, 72, 1721–1733. <https://doi.org/10.1016/j.jaridenv.2008.03.004>
- Scanlon, B. R., Keese, K. E., Flint, A. L., Flint, L. E., Gaye, C. B., Edmunds, W. M., & Simmers, I. (2006). Global synthesis of groundwater recharge in semiarid and arid regions. *Hydrological Processes*, 20(15), 3335–3370. <https://doi.org/10.1002/hyp.6335>
- Song, L., Liu, S., Kustas, W. P., Zhou, J., Xu, Z., Xia, T., & Li, M. (2016). Application of remote sensing-based two-source energy balance model for mapping field surface fluxes with composite and component surface temperatures. *Agricultural and Forest Meteorology*, 230–231, 8–19. <https://doi.org/10.1016/j.agrformet.2016.01.005>
- Taha, H., Akbari, H., & Rosenfeld, A. (1991). Heat island and oasis effects of vegetative canopies: Micro-meteorological field-measurements. *Theoretical and Applied Climatology*, 44, 123–138. <https://doi.org/10.1007/BF00867999>
- Wang Kaicun, Jiang Shaojing, Wang Jiankai, Zhou Chunlüe, Wang Xiaoyan, & Lee Xuhui. (2017). Comparing the diurnal and seasonal variabilities of atmospheric and surface urban heat islands based on the Beijing urban meteorological network. *Journal of Geophysical Research: Atmospheres*, 122(4), 2131–2154. <https://doi.org/10.1002/2016JD025304>
- Wang, L., Lee, X., Schultz, N., Chen, S., Wei, Z., Fu, C., ... Lin, G. (2018). Response of surface temperature to afforestation in the Kubuqi Desert, Inner Mongolia. *Journal of Geophysical Research*, (accepted). <https://doi.org/10.1002/2017JD027522>
- Wang, X., Yang, H., Shi, M., Zhou, D., & Zhang, Z. (2015). Managing stakeholders' conflicts for water reallocation from agriculture to industry in the Heihe River Basin in Northwest China. *Science of The Total Environment*, 505, 823–832. <https://doi.org/10.1016/j.scitotenv.2014.10.063>
- Wang, Y. Q., Xiong, Y. J., Qiu, G. Y., & Zhang, Q. T. (2016). Is scale really a challenge in evapotranspiration estimation? A multi-scale study in the Heihe oasis using thermal remote sensing and the three-temperature model. *Agricultural and Forest Meteorology*, 230–231, 128–141. <https://doi.org/10.1016/j.agrformet.2016.03.012>
- Wen, X., Yang, B., Sun, X., & Lee, X. (2016). Evapotranspiration partitioning through in-situ oxygen isotope measurements in an oasis cropland. *Agricultural and Forest Meteorology*, 230. <https://doi.org/10.1016/j.agrformet.2015.12.003>
- Working Group III. "Special Report on Climate Change, Desertification, Land Degradation, Sustainable Land Management, Food Security, and Greenhouse Gas Fluxes in Terrestrial Ecosystems." London: Intergovernmental Panel on Climate Change, 2017.
- Xiao, S., Xiao, H., Kobayashi, O., & Liu, P. (2007). Dendroclimatological Investigations of Sea Buckthorn (*Hippophae rhamnoides*) and Reconstruction of the Equilibrium Line Altitude of

- the July First Glacier in the Western Qilian Mountains, Northwestern China. *Tree-Ring Research*, 63(1), 15–26. <https://doi.org/10.3959/1536-1098-63.1.15>
- Xu, H., Sui, L., Yuhong, L., & Zhang, D. (2014). The Role of Water Users Associations in Integrated Water Resource Management of Zhangye City in Heihe River Basin, China. In V. R. Squires, H. M. Milner, & K. A. Daniell (Eds.), *River Basin Management in the Twenty-first Century* (pp. 304–324). CRC Press.
- Yuan, G., Zhang, L., Liang, J., Cao, X., Liu, H., & Yang, Z. (2017). Understanding the Partitioning of the Available Energy over the Semi-Arid Areas of the Loess Plateau, China. *Atmosphere*, 8(5), 87. <https://doi.org/10.3390/atmos8050087>
- Zhang, A., Zheng, C., Wang, S., & Yao, Y. (2015). Analysis of streamflow variations in the Heihe River Basin, northwest China: Trends, abrupt changes, driving factors and ecological influences. *Journal of Hydrology: Regional Studies*, 3, 106–124. <https://doi.org/10.1016/j.ejrh.2014.10.005>
- Zhang, B., & He, C. (2016). A modified water demand estimation method for drought identification over arid and semiarid regions. *Agricultural and Forest Meteorology*, 230–231, 58–66. <https://doi.org/10.1016/j.agrformet.2015.11.015>
- Zhao, L., Lee, X., & Liu, S. (2013). Correcting surface solar radiation of two data assimilation systems against FLUXNET observations in North America. *Journal of Geophysical Research (Atmospheres)*, 118, 9552–9564. <https://doi.org/10.1002/jgrd.50697>
- Zhu, G.-F., Zhang, K., Li, X., Liu, S.-M., Ding, Z.-Y., Ma, J.-Z., ... He, J.-H. (2016). Evaluating the complementary relationship for estimating evapotranspiration using the multi-site data across north China. *Agricultural and Forest Meteorology*, 230–231, 33–44. <https://doi.org/10.1016/j.agrformet.2016.06.006>